

Spring 2010

## Theoretical and computational study of time dependent scattering on a 2D surface

Michael Sohn  
*University of Nevada Las Vegas*

Follow this and additional works at: <https://digitalscholarship.unlv.edu/thesesdissertations>



Part of the [Quantum Physics Commons](#)

---

### Repository Citation

Sohn, Michael, "Theoretical and computational study of time dependent scattering on a 2D surface" (2010). *UNLV Theses, Dissertations, Professional Papers, and Capstones*. 16.  
<https://digitalscholarship.unlv.edu/thesesdissertations/16>

This Thesis is protected by copyright and/or related rights. It has been brought to you by Digital Scholarship@UNLV with permission from the rights-holder(s). You are free to use this Thesis in any way that is permitted by the copyright and related rights legislation that applies to your use. For other uses you need to obtain permission from the rights-holder(s) directly, unless additional rights are indicated by a Creative Commons license in the record and/or on the work itself.

This Thesis has been accepted for inclusion in UNLV Theses, Dissertations, Professional Papers, and Capstones by an authorized administrator of Digital Scholarship@UNLV. For more information, please contact [digitalscholarship@unlv.edu](mailto:digitalscholarship@unlv.edu).

THEORETICAL AND COMPUTATIONAL STUDY OF TIME  
DEPENDENT SCATTERING ON A 2D SURFACE

by

Michael Sohn

Bachelor of Science  
University of Nevada, Las Vegas  
2007

A thesis submitted in partial fulfillment of  
the requirements for the

**Master of Science in Physics**  
**Department of Physics and Astronomy**  
**College of Sciences**

**Graduate College**  
**University of Nevada, Las Vegas**  
**May 2010**

Copyright by Michael Sohn 2010  
All Rights Reserved



THE GRADUATE COLLEGE

We recommend the thesis prepared under our supervision by

**Michael Sohn**

entitled

**Theoretical and Computational Study of Time Dependent Scattering on a 2D Surface**

be accepted in partial fulfillment of the requirements for the degree of

**Master of Science in Physics**

Physics and Astronomy

Bernard Zygelman, Committee Co-chair

Tao Pang, Committee Co-chair

Stephen Lepp, Committee Member

Kathleen Robins, Graduate Faculty Representative

Ronald Smith, Ph. D., Vice President for Research and Graduate Studies  
and Dean of the Graduate College

**May 2010**

ABSTRACT

**THEORETICAL AND COMPUTATIONAL STUDY OF TIME  
DEPENDENT SCATTERING ON A 2D SURFACE**

by

Michael Sohn

Dr. Bernard Zygelman, Examination Committee Chair

Professor of Physics

University of Nevada, Las Vegas

The quantum mechanical treatment of the elastic scattering of atoms from a crystal surface provides valuable information, such as surface properties and gas-surface interaction potentials. However, since it is based on the stationary state solution, it does not provide the details of the scattering process in the neighborhood of the surface, especially when atoms are physically adsorbed.

In this thesis, the time evolution of the scattering process is treated in 2D with a model potential,  $V(x, z) = -|g|\delta(z) + \lambda\delta(z)\cos(2\pi x/a)$ , using the Gaussian wave packet approach. The focus is on the case where the Gaussian wave packet makes a transition into a selective adsorption state because it can provide information on the probability density of selectively adsorbed particles as well as the details of the scattering process in the neighborhood of the surface. The obtained Gaussian wave packet solution shows a transition into a selective adsorption state. However, the probability density of selectively adsorbed particles cannot be accurately determined because the Gaussian wave packet constructed from the Born approximate time-independent wave function does not conserve the total probability density.

## TABLE OF CONTENTS

ABSTRACT .....	iii
LIST OF FIGURES .....	v
ACKNOWLEDGEMENTS .....	vi
CHAPTER 1 INTRODUCTION AND OUTLINE .....	1
CHAPTER 2 THEORETICAL BACKGROUNDS .....	6
Lippmann-Schwinger Equation .....	6
Green's Function .....	7
Gaussian Wave Packet .....	8
CHAPTER 3 PARTICLE-SURFACE ELASTIC SCATTERING .....	10
Particle-Surface Interaction Potential .....	10
Diffraction Intensities .....	11
Selective Adsorption .....	12
Empirical Potential for H <sub>2</sub> -Graphite Surface .....	15
CHAPTER 4 CLASSICAL SCATTERING THEORY .....	19
One Scatterer .....	19
Periodic Scatterers .....	24
CHAPTER 5 QUANTUM SCATTERING IN 1D .....	26
Time Independent Wave Function .....	27
Time Dependent Wave Function .....	31
Graphical Description of Wave Packet .....	34
CHAPTER 6 QUANTUM SCATTERING IN 2D .....	41
Time Independent Wave Function .....	41
Time Dependent Wave Function .....	50
Graphical Description .....	52
Conclusions .....	57
APPENDIX A CALCULUS OF RESIDUES .....	58
APPENDIX B BOUND-STATE WAVE FUNCTION FOR $\delta$ POTENTIAL ...	60
APPENDIX C SOURCE CODE FOR NUMERICAL CALCULATION .....	62
BIBLIOGRAPHY .....	69
VITA .....	74

## LIST OF FIGURES

Figure 4.1	The effective potential for the interaction between a pair of neutral particles for various impact parameter values as a function of distance between the neutral particles. For the curve A bound states exist only if the energy is negative. For the curve B bound states exist even if the energy is positive. for the curve C no bound state exists. ....	21
Figure 4.2	The effective potential B with various energies of the incident particle. If $T_0 = V_1$ or $T_0 = V_3$ , the incident particle cannot be bound. If $T_0 = V_2$ , the particle can bound in the region $r_1 \leq r \leq r_2$ . ....	21
Figure 4.3	The trajectories of the incident hydrogen molecule at different impact parameters with $T_0 = 1.29$ meV. ....	23
Figure 4.4	The trajectories of the incident hydrogen molecule in the one-dimensional lattice of carbon atoms at different impact parameters with $T_0 = 1.29$ meV. ....	24
Figure 5.1	The two-dimensional system used in this thesis. $k_x$ and $k_z$ are the $x$ and $z$ components of the incident wave vector, and $k'_x$ and $k'_z$ are the $x$ and $z$ components of the diffracted wave vector. ....	26
Figure 5.2	The time dependence of the width of the Gaussian wave packet.	36
Figure 5.3	The Gaussian wave packet for $^1\text{H}_2$ at the temperature of 10 °K with $ g  = 0.144$ meV·Å at different times. ....	37
Figure 5.4	The Gaussian wave packet for $^1\text{H}_2$ at the temperature of 10 °K with $ g  = 1.440$ meV·Å at different times. ....	38
Figure 5.5	The Gaussian wave packet for $^1\text{H}_2$ at the temperature of 10 °K with $ g  = 14.40$ meV·Å at different times. ....	39
Figure 6.1	The diagram for computer simulation setup. $k_i = 1.12$ Å <sup>-1</sup> and $\theta_i = 12.94^\circ$ . ....	53
Figure 6.2	The density plots of the 2D Gaussian wave packets at different times for $^1\text{H}_2$ with $ g  = 3.96$ meV·Å, $k_i = 1.12$ Å <sup>-1</sup> and $\theta_i = 12.94^\circ$ . With these values the kinematic condition of selective adsorption is satisfied. The periodic potential site lies on $z = 0$ , but is not shown. ....	54
Figure 6.3	The density plots of the 2D Gaussian wave packets at different times for $^1\text{H}_2$ with $ g  = 3.96$ meV·Å, $k_i = 1.12$ Å <sup>-1</sup> and $\theta_i = 38.82^\circ$ . This incident angle does not satisfy the kinematic condition of selective adsorption with the given values of $ g $ and $k_i$ . The periodic potential site lies on $z = 0$ , but is not shown. ....	55
Figure 6.4	The density plots of the 2D Gaussian wave packets at different times for $^1\text{H}_2$ with $ g  = 3.96$ meV·Å, $k_i = 1.12$ Å <sup>-1</sup> and $\theta_i = 64.70^\circ$ . This incident angle does not satisfy the kinematic condition of selective adsorption with the given values of $ g $ and $k_i$ . The periodic potential site lies on $z = 0$ , but is not shown. ....	56

## ACKNOWLEDGEMENTS

I would like to show my sincere gratitude to my advisor Dr. Bernard Zygelman for his continuous support and encouragement. Without his help I could not have completed this work. I would also like to thank the members of my committee: Dr. Tao Pang, Dr. Stephen Lepp and Dr. Kathleen A. Robins.

I gratefully acknowledge the financial support for my graduate studies. This work has been partly supported by DE-FG36-05GO85028 and a NASA EPSCoR grant to the state of Nevada.

Lastly, I would like to thank my family for unconditional love and support.



## CHAPTER 1

### INTRODUCTION AND OUTLINE

Hydrogen has significant potential as a future energy carrier for mobile applications because of its sustainability and cleanness, but its use as an energy carrier is limited by hydrogen storage problems [1–3]. The current established storage systems for hydrogen, liquefaction and gas compression, are too bulky, economically inefficient and unsafe [4]. One of the more promising proposed solutions to these problems is the storage of molecular hydrogen on a surface of carbonaceous materials, either by chemisorption or physisorption.

Chemisorption is adsorption that results from a strong interaction, such as ionic bond or covalent bond, between an adsorbed particle and the surface of a solid. It occurs at certain adsorption sites on the surface so it takes place only in a monolayer. In chemisorption, the electronic structure of adsorbed particles is altered so the original adsorbed particles can only be recovered at high temperature on desorption. For instance, chemically bonded hydrogen to single-walled carbon nanotubes requires a temperature greater than 600 K to desorb [3].

Another method, physisorption, results from the weak intermolecular interaction between an adsorbed particle and the surface of a solid, and can take place in multilayers under appropriate conditions. The weak intermolecular interaction barely alters the electronic structure of physically adsorbed particles so the original adsorbed particles can be easily recovered on desorption. Because of this reversibility, for the application of mobile hydrogen storage systems, physisorption would be preferable to chemisorption because adsorbed hydrogen must be easily accessible for delivery. There have been numerous studies on hydrogen physisorption on various carbonaceous materials, and high hydrogen storage capacities of those materials at room temperature and atmospheric pressure have been reported in the literature [5–8]. However, their values could not be confirmed by other researchers experimentally [9–11] nor

computationally [12–15], leaving room for further research on this topic.

In the development of a new storage device, information on the surface properties of the material and the gas-surface interaction potential is essential, and such information is obtained from gas-surface scattering studies [16, 17]. Therefore, an intimate knowledge of gas-solid scattering theories is critical, and should be based on quantum mechanics for the hydrogen storage because the de Broglie wave length of the hydrogen molecule, particularly at low temperature, is on the order of the intermolecular force as well as the crystal lattice parameters [18], where classical scattering theory fails.

The early work of Lennard-Jones and Devonshire [19–21] developed a quantum mechanical elastic scattering theory to explain the so-called “selective adsorption” state, in which the particle is bound to the surface in the perpendicular direction while it is free to translate in the direction parallel to the surface [17]. Particles in this bound state cause minima in the specular intensity of the incident beam of particles. The measurements of these minima can be used to determine the laterally averaged gas-surface potential, and those for many different gas-solid systems have been successfully obtained [22–29]. For gas-surface diffraction, various quantum mechanical approaches have been proposed: the close coupling formulation by Tsuchida [18] and Wolken [30], the Cabrera-Celli-Goodman-Manson (CCGM) theory by Cabrera et al. [31], the Born series approach by Armand et al. [32] and the hard corrugated surface model approach by Garibaldi et al. [33]. These approaches have been applied to many gas-solid systems [34], especially the He-LiF system [35–37], and qualitative agreement with experimental results [34, 38–42] has been made.

The solutions obtained by those approaches are time-independent wave functions. These stationary wave functions can provide general properties of the gas-surface system, such as the diffraction intensity and the gas-surface potential. However, they cannot describe the scattering process as it actually occurs because both the incident

and scattered waves appear and both waves are spread out over the entire surface. In this thesis, we attempt to provide a time-dependent solution of the gas-surface scattering in 2D, and graphically describe the time evolution of the scattering process, especially when the incident particle makes a transition into a selective adsorption state. Because the particle at very far away from the surface behaves just like a free particle and in reality incident particles possess a distribution of momenta due to the experimental limit in obtaining monoenergetic particles, the time-dependent Gaussian wave packet approach is employed with a model potential given by

$$V(x, z) = -|g|\delta(z) + \lambda\delta(z) \cos(2\pi x/a), \quad (1.1.1)$$

where  $g$  and  $\lambda$  are constants, and  $a$  is the distance between the interaction sites. This simplified version of the general form of periodic potentials is chosen because it possesses properties of the realistic gas-surface potential necessary for the study of the scattering process, and allows us to obtain an analytic expression for the kinematic condition of selective adsorption. Also, it can reproduce any bound state of realistic potentials by adjusting the value of  $|g|$  because the delta function potential has one and only one bound state.

In chapter 2 the fundamental mathematical tools for quantum mechanical scattering theory are covered. The Lippmann-Schwinger Equation is reviewed in section 2.1, and Green's function for the Helmholtz equation in section 2.2. The rationale for using the Gaussian wave packet in the development of the time-dependent wave function is given in section 2.3.

In chapter 3 the quantum theory and its application to the elastic scattering in the gas-surface system is reviewed. In section 3.1 the general form of the periodic potential for the gas-surface interaction is considered. In section 3.2 coupled differential equations, which result from periodicity of the wave function, are reviewed to describe the diffraction intensity. In section 3.3 selective adsorption is described and

the kinematic condition for selective adsorption is reviewed. How selective adsorption measurements are used to obtain bound state energy levels is also covered. In section 3.4 the method used in determining the laterally averaged interaction potential for  $\text{H}_2$  on the (0001) graphite surface published by Mattera et al. [27] is reviewed. Then, with the determined potential, energy levels for  $^1\text{H}_2$  and  $^2\text{H}_2$  are calculated using the self-consistent field (SCF) method to describe how to determine the laterally averaged potential with the measurements of selective adsorption.

In chapter 4 the classical scattering in 2D is treated to gain some insight into the scattering process. In section 4.1, the scattering of an incident particle on single scattering center is treated, especially in the quasi-bound state. In section 4.2, an incident particle on a one-dimensional lattice of scattering centers is considered in order to graphically describe the classical analogue of “selective adsorption”. In the calculation,  $\text{H}_2$  is the incident particle, C refers to scattering centers and a Lennard-Jones potential for the interaction potential between them is used.

In chapter 5 the quantum scattering in 1D is treated because the two-dimensional Schrödinger equation can be separated into two one-dimensional Schrödinger equations if the potential depends only on one variable. In section 5.1 the time-independent wave function for the laterally averaged potential,  $w_0 = -|g|\delta(z)$ , is obtained by solving the Lippmann-Schwinger equation, and the transmission and the reflection amplitudes are obtained. Energy eigenvalues for the laterally averaged potential are also obtained in order to determine the kinematic condition for selective adsorption in the two-dimensional system treated in chapter 6. In section 5.2 the Gaussian wave packet solution of the Schrödinger equation with the laterally averaged potential is obtained in a closed-form expression. In section 5.3 the dispersion rate for the Gaussian wave packet is calculated to obtain the optimum initial width, and the wave packets with different values of parameters are plotted to visualize the scattering process in the neighborhood of the interaction site. The validity of the graphical description is also

verified.

In chapter 6 the two-dimensional elastic scattering of a particle in the periodic potential is treated. In section 6.1 the time-independent wave function is first obtained using the Born approximation because the exact wave function cannot be obtained due to the periodic term in the model potential Eq. (1.1.1). Then, the kinematic condition for selective adsorption is deduced from this wave function. It is also shown that the wave function in a bound state satisfies the diffraction condition. In section 6.2 the Gaussian wave packet is constructed with the obtained Born approximate time-independent wave function. In section 6.3 the Gaussian wave packets with different incident angles are plotted to visually describe selective adsorption. In section 6.4 conclusions are presented.

CHAPTER 2  
THEORETICAL BACKGROUNDS

2.1 Lippmann-Schwinger Equation

For the Hamiltonian

$$\hat{H} = \hat{H}_0 + \hat{V}, \quad (2.1.1)$$

where  $\hat{H}_0$  is the free-particle Hamiltonian, the solution to the Schrödinger equation can be given by [43]

$$|\psi^{(+)}\rangle = |\phi\rangle + \frac{1}{E - \hat{H}_0 + i\epsilon} V |\psi^{(+)}\rangle, \quad (2.1.2)$$

where  $\epsilon$  is a positive infinitesimal,  $|\phi\rangle$  is an incident wave and  $|\psi^{(+)}\rangle$  is an outgoing scattered wave. This is the Lippmann-Schwinger equation and is independent of particular representations. The coordinate representation can be obtained by multiplying by a coordinate eigenbra  $\langle \mathbf{r} |$ . That is,

$$\langle \mathbf{r} | \psi^{(+)} \rangle = \langle \mathbf{r} | \phi \rangle + \frac{2m}{\hbar^2} \int d^n r' G(\mathbf{r}, \mathbf{r}') \langle \mathbf{r}' | V | \psi^{(+)} \rangle, \quad (2.1.3)$$

where  $m$  is the particle mass,  $n$  is dimension of  $\mathbf{r}$  and  $G(\mathbf{r}, \mathbf{r}')$  is a Green's function defined by

$$G(\mathbf{r}, \mathbf{r}') = \frac{\hbar^2}{2m} \left\langle \mathbf{r} \left| \frac{1}{E - \hat{H}_0 + i\epsilon} \right| \mathbf{r}' \right\rangle, \quad (2.1.4)$$

which satisfies

$$(\nabla^2 + k^2) G(\mathbf{r}, \mathbf{r}') = \delta^n(\mathbf{r} - \mathbf{r}'), \quad (2.1.5)$$

where  $k = \sqrt{2mE}/\hbar$ . For a local potential that depends only on the position, we can write that

$$\langle \mathbf{r}' | V | \psi^+ \rangle = V(\mathbf{r}') \langle \mathbf{r}' | \psi^+ \rangle. \quad (2.1.6)$$

Thus, for a local potential Eq. (2.1.3) can be given by

$$\langle \mathbf{r} | \psi^{(+)} \rangle = \langle \mathbf{r} | \phi \rangle + \frac{2m}{\hbar^2} \int d^n r' G(\mathbf{r}, \mathbf{r}') V(\mathbf{r}') \langle \mathbf{r}' | \psi^+ \rangle. \quad (2.1.7)$$

This integral equation has advantage over the differential form of the Schrödinger equation in studying scattering problems since it incorporates the boundary conditions explicitly.

## 2.2 Green's Function

The free-particle Hamiltonian  $\hat{H}_0$  is given by

$$\hat{H}_0 = \frac{\hat{\mathbf{p}}^2}{2m}. \quad (2.2.1)$$

Thus, the Green's function for the Helmholtz equation Eq. (2.1.4) becomes

$$G(\mathbf{r}, \mathbf{r}') = \frac{\hbar^2}{2m} \left\langle \mathbf{r} \left| \frac{1}{E - \hat{\mathbf{p}}^2/2m + i\epsilon} \right| \mathbf{r}' \right\rangle. \quad (2.2.2)$$

By inserting closure after  $\langle \mathbf{r} |$  and before  $|\mathbf{r}' \rangle$  Eq. (2.2.2) becomes

$$G(\mathbf{r}, \mathbf{r}') = \frac{\hbar^2}{2m} \int d^n p \int d^n p' \langle \mathbf{r} | \mathbf{p} \rangle \left\langle \mathbf{p} \left| \frac{1}{E - \hat{\mathbf{p}}^2/2m + i\epsilon} \right| \mathbf{p}' \right\rangle \langle \mathbf{p}' | \mathbf{r}' \rangle, \quad (2.2.3)$$

where  $n$  is dimension of  $\mathbf{p}$ . The first term of the integrand  $\langle \mathbf{r} | \mathbf{p} \rangle$  and the third term  $\langle \mathbf{p}' | \mathbf{r}' \rangle$  are given by [43]

$$\langle \mathbf{r} | \mathbf{p} \rangle = \frac{e^{i\mathbf{p}\cdot\mathbf{r}/\hbar}}{(2\pi\hbar)^{n/2}}, \quad (2.2.4)$$

and

$$\langle \mathbf{p}' | \mathbf{r}' \rangle = \frac{e^{-i\mathbf{p}'\cdot\mathbf{r}'/\hbar}}{(2\pi\hbar)^{n/2}}. \quad (2.2.5)$$

With these equations Eq. (2.2.3) after applying  $\hat{\mathbf{p}}^2$  on  $\langle \mathbf{p} |$  becomes

$$G(\mathbf{r}, \mathbf{r}') = \frac{\hbar^2}{2m(2\pi\hbar)^n} \int d^n p \frac{e^{i\mathbf{p}\cdot(\mathbf{r}-\mathbf{r}')/\hbar}}{(E - \mathbf{p}^2/2m + i\epsilon)}. \quad (2.2.6)$$

It is common to use the wave vector  $\mathbf{k}$  rather than the momentum vector  $\mathbf{p}$ . Thus,

with the relation  $\mathbf{p} = \hbar\mathbf{k}$ , the Green's function Eq. (2.2.6) can be given by

$$G(\mathbf{r}, \mathbf{r}') = \frac{\hbar^2}{2m(2\pi)^n} \int d^n k \frac{e^{i\mathbf{k}(\mathbf{r}-\mathbf{r}')}}{E - (\hbar\mathbf{k})^2/2m + i\epsilon}. \quad (2.2.7)$$

### 2.3 Gaussian Wave Packet

By attaching the standard time dependence,  $e^{iEt/\hbar}$ , to the time-independent wave function for a free particle, the time-dependent wave function for a free particle can be given by

$$\psi(\mathbf{r}, t) = Ae^{i(\mathbf{k}\cdot\mathbf{r}-\omega t)}, \quad (2.3.1)$$

where  $\omega = E/\hbar$ . The physical interpretation of the wave function is that  $|\psi(\mathbf{r}, t)|^2$  is the probability density for finding the particle at position  $\mathbf{r}$ , at time  $t$ . However, the modulus squared of Eq. (2.3.1) is  $|A|^2$ , which doesn't depend on  $\mathbf{r}$  nor  $t$ . In other words, a particle is equally probable to be found anywhere at all times, and the wave function Eq. (2.3.1) cannot represent physically realizable state. We therefore construct a wave packet by taking a linear combination of such states with a distribution of momenta that localize the particle in space:

$$\Psi(\mathbf{r}, t) = \int_{-\infty}^{\infty} d^n k \Phi(\mathbf{k} - \mathbf{k}_0) e^{i(\mathbf{k}\cdot\mathbf{r}-\omega t)}, \quad (2.3.2)$$

where  $\mathbf{k}_0$  is the initial wave vector. This wave packet can be normalized for appropriate  $\Phi(\mathbf{k} - \mathbf{k}_0)$ , and the Gaussian distribution is used in this thesis because it gives the minimum-uncertainty. The Gaussian wave packet for free particles is given by

$$\Psi(\mathbf{r}, t) = N \int_{-\infty}^{\infty} d^n k \exp\left[-\frac{(\mathbf{k} - \mathbf{k}_0)^2}{2\sigma_k^2}\right] \exp[i\mathbf{k} \cdot \mathbf{r}] \exp\left[-i\frac{\hbar k^2 t}{2m}\right], \quad (2.3.3)$$

where  $N$  is a normalization factor, and  $\sigma_k$  is the width of the wave packet in  $\mathbf{k}$  space.

Far from the surface the incident and scattered particles behave like free particles, and in reality incident particles possess a distribution of momenta due to the experimental limit in obtaining monoenergetic particles so the incident particles should



be represented by wave packets of finite uncertainty in momentum. Thus, the wave packet solution should be used for the time-dependent solution of the gas-surface scattering. The wave packet for scattering with the same Gaussian weight used for the free particle is given by

$$\Psi(\mathbf{r}, t) = N \int_{-\infty}^{\infty} d^n k \exp \left[ -\frac{(\mathbf{k} - \mathbf{k}_0)^2}{2\sigma_k^2} \right] \psi_s(\mathbf{r}) \exp \left[ -i\frac{\hbar k^2 t}{2m} \right], \quad (2.3.4)$$

where  $\psi_s(\mathbf{r})$  is the time-independent wave function for scattering.

## CHAPTER 3

### PARTICLE-SURFACE ELASTIC SCATTERING

#### 3.1 Particle-Surface Interaction Potential

Solids are composed of a periodic array of atoms. Thus, when a particle approaches the surface of a solid it experiences a periodic potential caused by an atom or a group of atoms attached to every repeating point, lattice point. Here we review the potential appropriate for particle-surface interactions due to this periodicity.

If we define a two-dimensional lattice vector  $\mathbf{L}$  parallel to the surface such that

$$\mathbf{L} = l_1 \mathbf{a}_1 + l_2 \mathbf{a}_2, \quad (3.1.1)$$

where  $l_1$  and  $l_2$  are integers, and  $\mathbf{a}_1$  and  $\mathbf{a}_2$  are translation vectors so defined that the atomic arrangement at one position is identical to that at another position translated by  $\mathbf{L}$ . Then, for an infinite planar surface,

$$V(\mathbf{r}) = V(\mathbf{r} + \mathbf{L}). \quad (3.1.2)$$

This periodicity allows us to express  $V(\mathbf{r})$  as a Fourier series [44]:

$$V(z, \mathbf{R}) = \sum_{\mathbf{G}} w_{\mathbf{G}}(z) e^{i\mathbf{G} \cdot \mathbf{R}}, \quad (3.1.3)$$

where  $\mathbf{R}$  is a two-dimensional position vector parallel to the surface, and  $\mathbf{G}$  is a two-dimensional vector defined by

$$\mathbf{G} = g_1 \mathbf{b}_1 + g_2 \mathbf{b}_2, \quad (3.1.4)$$

where  $g_1$  and  $g_2$  are integers, and  $\mathbf{b}_1$  and  $\mathbf{b}_2$  are reciprocal vectors defined by

$$\mathbf{a}_i \cdot \mathbf{b}_j = 2\pi \delta_{ij}, \quad (3.1.5)$$

where  $\delta_{ij} = 1$  if  $i = j$ , and  $\delta_{ij} = 0$  if  $i \neq j$ . By placing the origin of  $\mathbf{R}$  at the center of inversion symmetry so that  $w_{\mathbf{G}}(z) = w_{-\mathbf{G}}(z)$  [44], the general form of the potential for the particle-surface interaction  $V(\mathbf{r})$  can be given by

$$V(z, \mathbf{R}) = w_0(z) + 2 \sum_{\mathbf{G} > 0} w_{\mathbf{G}}(z) \cos(\mathbf{G} \cdot \mathbf{R}). \quad (3.1.6)$$

### 3.2 Diffraction Intensities

As a result of periodicity of the solid surface, the wave function  $\Psi(\mathbf{r})$  can be expanded by Bloch's theorem into the form

$$\Psi(\mathbf{r}) = \sum_{\mathbf{G}} \psi_{\mathbf{G}}(z) e^{i(\mathbf{K} + \mathbf{G}) \cdot \mathbf{R}}, \quad (3.2.1)$$

where  $\mathbf{K}$  is a two dimensional vector consisting of the  $x$  and  $y$  components of an incident wave vector  $\mathbf{k}$ . Then, after differentiation the Schrödinger equation for a particle of mass  $m$  and wave incident vector  $\mathbf{k}$  in the periodic potential  $V(\mathbf{r})$  can be given by

$$\left[ \frac{d^2}{dz^2} + k^2 - (\mathbf{K} + \mathbf{G})^2 - \frac{2m}{\hbar^2} \sum_{\mathbf{G}'} w_{\mathbf{G}'}(z) e^{i\mathbf{G}' \cdot \mathbf{R}} \right] \sum_{\mathbf{G}} \psi_{\mathbf{G}}(z) e^{i(\mathbf{K} + \mathbf{G}) \cdot \mathbf{R}} = 0. \quad (3.2.2)$$

If both sides of Eq. (3.2.2) are multiplied by  $e^{-i(\mathbf{K} + \mathbf{G}'') \cdot \mathbf{R}}$  and integrated over the two dimensional unit cell, it becomes

$$\left( \frac{d^2}{dz^2} + k_{\mathbf{G}z}^2 \right) \psi_{\mathbf{G}}(z) = \frac{2m}{\hbar^2} \sum_{\mathbf{G}'} w_{\mathbf{G} - \mathbf{G}'} \psi_{\mathbf{G}'}(z), \quad (3.2.3)$$

where

$$k_{\mathbf{G}z}^2 = k^2 - (\mathbf{K} + \mathbf{G})^2. \quad (3.2.4)$$

This infinite set of coupled differential equations has two different types of solution: “open channel” solution and “closed channel” solution. An open channel representing a diffracted partial wave that can be observed at large  $z$  occurs when  $k_{\mathbf{G}z}^2 > 0$  and a closed channel corresponding to a surface partial wave that decays exponentially normal to the surface occurs when  $k_{\mathbf{G}z}^2 < 0$ . In general, this infinite set of coupled differential equations is approximated by a finite number of channels, and the solution

for each channel is computed by imposing appropriate boundary conditions:

$$\psi_{\mathbf{G}}(z) \xrightarrow{z \rightarrow \infty} 0 \quad (3.2.5)$$

for closed channels, and

$$\psi_{\mathbf{G}}(z) \xrightarrow{z \rightarrow \infty} N [\delta_{\mathbf{G},0} e^{-ik_z z} + S_{\mathbf{G}} e^{ik_{\mathbf{G}z} z}], \quad (3.2.6)$$

for open channels, where  $N$  is a normalization factor,  $\delta_{\mathbf{G},0}$  is the Kronecker delta function and  $S_{\mathbf{G}}$  is a constant. This constant  $S_{\mathbf{G}}$  is related to the diffraction intensity  $I_{\mathbf{G}}$ , which is defined as the outgoing flux relative to the incident flux, such that [44]

$$I_{\mathbf{G}} = \left( \frac{k_{\mathbf{G}z}}{k_z} \right) |S_{\mathbf{G}}|^2. \quad (3.2.7)$$

In elastic scattering, the sum of intensities over all allowed diffracted particles should be unity:

$$\sum_{\mathbf{G}} I_{\mathbf{G}} = 1. \quad (3.2.8)$$

### 3.3 Selective Adsorption

When a particle interacts with the potential at the surface, it may make an elastic transition into the so-called “selective adsorption” state in which the particle is bound to the surface in the perpendicular direction while it is free to translate in the direction parallel to the surface [17]. This transition occurs when the particle’s energy associated with its motion in the direction perpendicular to the surface is equal to one of bound state energies of the potential  $\omega_0(z)$  in Eq. (3.1.6) [45].

According to Bloch’s theorem, the wave function in a periodic potential can be given by

$$\Psi(\mathbf{r}) = \sum_{\mathbf{G}} \psi_{\mathbf{G}}(z) e^{i(\mathbf{K}_i + \mathbf{G}) \cdot \mathbf{R}}, \quad (3.3.1)$$

where  $z$  is taken as the outward normal direction to the surface plane. Far from the

surface the diffracted particle behaves like a free particle so it can be expressed by

$$\lim_{z \rightarrow \infty} \Psi_r(\mathbf{r}) = A_{\mathbf{G}} e^{ik_{rz}z} e^{i\mathbf{K}_r \cdot \mathbf{R}}, \quad (3.3.2)$$

where  $A_{\mathbf{G}}$  is a constant. From Equations (3.3.1) and (3.3.2) the values of  $\mathbf{K}_r$  is restricted such that

$$\mathbf{K}_r = \mathbf{K}_i + \mathbf{G}. \quad (3.3.3)$$

In elastic scattering the total energy should be conserved. Thus,

$$k_{rz}^2 + k_{rx}^2 + k_{ry}^2 = k_{iz}^2 + k_{ix}^2 + k_{iy}^2. \quad (3.3.4)$$

These two conditions, the conservation of momentum parallel to the surface and conservation of total energy, provide the kinematic conditions for selective adsorption.

In the zeroth-order approximation, the selectively adsorbed particle may be treated as a free-particle in its translation parallel to the surface, or the Fourier expansion of the particle-surface interaction potential Eq. (3.1.6) can be reduced to

$$V(\mathbf{r}) \approx w_0(z). \quad (3.3.5)$$

Then, the diffracted particle energy associated with the motion parallel to the surface can be given by

$$E_{\mathbf{K}_r} = \frac{\hbar^2}{2m} \mathbf{K}_r^2. \quad (3.3.6)$$

Thus, from the conservation of momentum parallel to the surface and conservation of total energy, Eq. (3.3.3) and (3.3.4), the kinematic condition for selective adsorption can be obtained such that

$$\frac{\hbar^2}{2m} (k_{iz}^2 + K_i^2) = E_n + \frac{\hbar^2}{2m} (\mathbf{K}_i + \mathbf{G})^2. \quad (3.3.7)$$

This condition indicates that the changes in the kinetic energy associated with motion parallel to the surface is  $(\mathbf{K}_i + \mathbf{G})^2 - K_i^2$ . For the case of positive  $\mathbf{G}$  or “forward

scattering” [44], the kinetic energy associated with motion parallel to the surface increases after the particle’s interaction with the surface so the energy associated with motion perpendicular to the surface should decrease. In particular, when  $(\mathbf{K}_i + \mathbf{G})^2 - K_i^2 > \hbar^2 k_{iz}^2/2m$ ,  $E_n$  must be negative. In other words, the particle is in a bound state in the direction perpendicular to the surface, or selectively adsorbed.

For an instance, in the case of a simple square lattice with lattice spacing  $a$ , such as LiF, the reciprocal vector  $\mathbf{G}$  is given by

$$\mathbf{G} = \frac{2g_1\pi}{a}\hat{\mathbf{x}} + \frac{2g_2\pi}{a}\hat{\mathbf{y}}. \quad (3.3.8)$$

Therefore, from Equations (3.3.3) and (3.3.4), the components of the diffracted wave vector are given by

$$k_{rx} = k_{ix} + \frac{2g_1\pi}{a}, \quad (3.3.9)$$

$$k_{ry} = k_{iy} + \frac{2g_2\pi}{a}, \quad (3.3.10)$$

$$k_{rz}^2 = k_{iz}^2 - \frac{4\pi}{a}(g_1k_{ix} + g_2k_{iy}) - \frac{4\pi^2}{a^2}(g_1^2 + g_2^2). \quad (3.3.11)$$

It is clear that the value of  $k_{rz}^2$  given by Eq. (3.3.11) becomes negative when  $g_1$  and  $g_2$  become large positive numbers. It is also possible to arrange the experiment to obtain the negative value of  $k_{rz}^2$  [44]. The negative value of  $k_{rz}^2$  implies that  $k_{rz}$  is imaginary so it can be expressed as

$$k_{rz} = i\kappa_{rz}, \quad (3.3.12)$$

where  $\kappa_{rz}$  is real and its magnitude is equal to that of  $k_{rz}$ . Thus, the diffracted wave function far from the surface can be given by

$$\lim_{z \rightarrow \infty} \Psi_r(\mathbf{r}) = S_{\mathbf{G}} e^{-\kappa_{rz}z} e^{i\mathbf{K}_r \cdot \mathbf{R}}. \quad (3.3.13)$$

This wave function approaches zero as  $z$  increases. That is, the incident particle is

bound in the  $z$ -direction while translating parallel to the surface.

In the experiment, the orientation of the beam of incident particles is generally given in terms of polar and azimuthal angles denoted by  $\theta_i$  and  $\phi_i$ , respectively [44] so that the components of the incident wave vector are given by

$$k_{iz} = -k_i \cos \theta_i, \quad (3.3.14)$$

$$k_{ix} = k_i \sin \theta_i \cos \phi_i, \quad (3.3.15)$$

$$k_{iy} = k_i \sin \theta_i \sin \phi_i, \quad (3.3.16)$$

where  $k_i$  is the magnitude of  $\mathbf{k}_i$  and  $0^\circ \leq \theta_i \leq 90^\circ$ . Thus, in the case of a simple square lattice with lattice spacing  $a$ , the kinematic condition for selective adsorption, Eq. (3.3.7) becomes

$$\left( \sin \theta_i \cos \phi_i + \frac{2g_1\pi}{ak_i} \right)^2 + \left( \sin \theta_i \sin \phi_i + \frac{2g_2\pi}{ak_i} \right)^2 = 1 + \frac{2m}{\hbar^2 k_i^2} |E_n|, \quad (3.3.17)$$

indicating that if the positions of all measured minima in the specular intensity are plotted in the plane  $(\sin \theta_i \cos \phi_i, \sin \theta_i \sin \phi_i)$ , the minima relative to  $E_n$  are on a circle centered at  $(-2g_1\pi/ak_i, -2g_2\pi/ak_i)$  and with radius  $[1 + (2m/\hbar^2 k_i^2)|E_n|]^{1/2}$ .

### 3.4 Empirical Potential for H<sub>2</sub>-Graphite Surface

From measurements of minima in the specular intensity associated with selective adsorption, eigenvalues of the  $z$ -dependent part of separated Schrödinger equation can be determined as described in the previous section. Using these eigenvalues, the laterally averaged potential  $w_0(z)$  can be obtained, and those for many different gas-solid systems have been obtained [22–29]. Here the work of Mattera et al. [27] is reviewed to study a method of obtaining the laterally averaged potential from the measurements of selective adsorption.

The proposed laterally averaged potential for H<sub>2</sub> on the (0001) graphite surface by Mattera et al. [27] is given by

$$w_0(z) = D \left[ \left(1 + \frac{\lambda z}{p}\right)^{-2p} - 2 \left(1 + \frac{\lambda z}{p}\right)^{-p} \right], \quad (3.4.1)$$

where  $D$  is the well depth,  $\lambda$  a range parameter and  $-1 \leq 1/p \leq 1$ . These three parameters are determined by minimizing the chi square test:

$$\chi^2 = \sum_n \left[ \frac{E_n^* - E_n(D, \lambda, p)}{\Delta_n} \right]^2, \quad (3.4.2)$$

where  $E_n^*$  is the experimental value for the  $n$ th energy level obtained from the measurements of selective adsorption,  $\Delta_n$  is its standard deviation and  $E_n(D, \lambda, p)$  is the  $n$ th eigenvalue of the Schrödinger equation for the proposed potential  $w_0(z)$ .

The Schrödinger equation for a particle with mass  $m$  in the proposed potential  $w_0(z)$  is given by

$$-\frac{\hbar^2}{2m} \frac{d^2}{dz^2} \psi(z) + w_0(z) \psi(z) = E_n \psi(z). \quad (3.4.3)$$

If we define  $\xi \equiv \lambda z$  and rearrange Eq. (3.4.3), the Schrödinger equation becomes

$$\frac{d^2}{d\xi^2} \psi(\xi) - \frac{2mD}{\hbar^2 \lambda^2} \left\{ \varepsilon_n + \left[ \left(1 + \frac{\xi}{p}\right)^{-2p} - 2 \left(1 + \frac{\xi}{p}\right)^{-p} \right] \right\} \psi(\xi) = 0, \quad (3.4.4)$$

where  $\varepsilon_n = -E_n/D$ . This equation cannot be solved for  $\varepsilon_n$  analytically except  $p = \pm 1$  and  $p = \infty$ . However, in the well-bottom region of the potential approximate equations for  $\varepsilon_n$  can be obtained by expanding  $w_0(z)/D$  in powers of  $\xi$  and using the Dunham equations, which is given by [46]

$$\begin{aligned} \varepsilon_n = & 1 - \frac{\delta}{A^2} - \left(1 - \frac{\delta}{A^2} \frac{S-1}{S}\right) \left(\frac{n+1/2}{A}\right) + \frac{S-1}{2S} \left(1 - \frac{\delta}{A^2} \frac{S-1}{S}\right) \left(\frac{n+1/2}{A}\right)^2 \\ & - \frac{(S-1)(S-2)}{6S^2} (1-B) \left(\frac{n+1/2}{A}\right)^3 + \dots, \end{aligned} \quad (3.4.5)$$

where



$$\delta = \frac{1 + 1/p}{32p}, \quad \frac{1}{S} = \frac{1}{2} - \frac{1}{4p} \left( 3 + \frac{1}{p} \right), \quad A = \frac{(2mD)^{1/2}}{2\hbar\lambda}, \quad (3.4.6)$$

and

$$B = \frac{1}{12} \frac{1 - 1/p}{1 + 1/3p} \left[ 1 + \frac{5}{4} \left( \frac{3}{2A} - \frac{1 - 1/p}{n + 1/2} \right) \frac{(1 + 1/2p)^{-1}}{n + 1/2} \right]. \quad (3.4.7)$$

This equation, in case  $\delta/A^2 \ll 1$ , concurs up to the quadratic term with the binomial expansion of [46]

$$\varepsilon_n^b = \left[ \left( 1 + \frac{\delta}{A^2} \right)^{-1/S} - \frac{n + 1/2}{AS} \right]^S. \quad (3.4.8)$$

The terms after the quadratic term of Eq. (3.4.8) are different from those of Eq. (3.4.5). However, the eigenvalues obtained from Eq. (3.4.8) is more accurate than from Eq. (3.4.5) over a wide energy range [46].

Replacing  $E_n(D, \lambda, p)$  in Eq. (3.4.2) with  $D\varepsilon_n^b$ , the three parameters  $D$ ,  $\lambda$  and  $p$  can be determined by minimizing  $\chi^2$ . The obtained values are  $D = 51.7$  meV,  $\lambda = 1.45 \text{ \AA}^{-1}$  and  $p = 3.9$  with  $\chi^2 = 1.7$ , and these values are identical to those obtained by Mattera et al. (However, their value for  $\chi^2$  is 5.5.) With these values the Schrödinger equation Eq. (3.4.4) can be given by

$$\frac{d^2}{d\xi^2} \psi(\xi) - 4A^2 \left\{ \varepsilon_n + \left[ \left( 1 + \frac{\xi}{3.9} \right)^{-7.8} - 2 \left( 1 + \frac{\xi}{3.9} \right)^{-3.9} \right] \right\} \psi(\xi) = 0, \quad (3.4.9)$$

where  $A$  is a unitless quantity defined in Eq. (3.4.6). This equation is solved numerically for the eigenvalues  $\varepsilon_n$  by the self-consistent field (SCF) method. The calculated energy levels for  $^1\text{H}_2$  and  $^2\text{H}_2$  are reported in Table 1, along with the measured energy levels, their standard deviation and the calculated energy levels reported by Mattera et al. [27].

Table 1

Energy eigenvalues for H<sub>2</sub>/(0001) graphite.

Isotope	n	E <sub>n</sub> <sup>*</sup> (meV) [27] (exptl.)	Δ <sub>n</sub> (meV) [27] (std. dev.)	E <sub>n</sub> (meV) (theo.)
<sup>1</sup> H <sub>2</sub>	0	-41.6	0.25	-41.75 (-41.75)
<sup>1</sup> H <sub>2</sub>	1	-26.4	0.25	-26.17 (-26.18)
<sup>1</sup> H <sub>2</sub>	2	-15.3	0.25	-15.29 (-15.30)
<sup>1</sup> H <sub>2</sub>	3	-7.9	0.25	-8.14 ( -8.15)
<sup>1</sup> H <sub>2</sub>	4	-3.6	0.25	-3.82 ( -3.82)
<sup>1</sup> H <sub>2</sub>	5	-1.4	0.25	-1.49 ( -1.49)
<sup>2</sup> H <sub>2</sub>	0	—	—	—
<sup>2</sup> H <sub>2</sub>	1	—	—	—
<sup>2</sup> H <sub>2</sub>	2	-23.1	0.25	-22.87 (-22.88)
<sup>2</sup> H <sub>2</sub>	3	-15.4	0.25	-15.54 (-15.55)
<sup>2</sup> H <sub>2</sub>	4	-10.0	0.25	-10.08 (-10.09)
<sup>2</sup> H <sub>2</sub>	5	-6.3	0.25	-6.19 ( -6.19)
<sup>2</sup> H <sub>2</sub>	6	-3.7	0.25	-3.53 ( -3.54)
<sup>2</sup> H <sub>2</sub>	7	-1.9	0.25	-1.83 ( -1.84)

The measured energy levels E<sub>n</sub><sup>\*</sup>, their standard deviation Δ<sub>n</sub>, and the calculated energy levels E<sub>n</sub> in the parenthesis are the values reported by Mattera et al.

## CHAPTER 4

### CLASSICAL SCATTERING THEORY

For light molecules, such as hydrogen molecules, the gas-surface scattering should be quantum mechanically treated, particularly when the temperature of molecules is low, because the de Broglie wave length of a gas molecule is on the order of the intermolecular forces and crystal lattice parameters [18]. However, classical scattering theory is relatively easy, and in many cases it provides a good approximation to the quantum dynamics. Moreover, even though selective adsorption is defined the quantum mechanical scattering, it has been conjectured that it is associated with classical trapping of the incident particle by the attractive well in the neighborhood of the surface [47]. Thus, we begin with classical scattering theory to gain some insight into the scattering process, especially when the incoming particle is physically adsorbed. We first treat classical scattering of two particles because trapping phenomena also occurs in the scattering of two particles so it can provide physical insight into trapping phenomena in the gas-surface system.

#### 4.1 One Scatterer

When a particle approaches a scattering center, its initial direction is altered by the interaction between them. For the case in which an incident particle and a scattering center are neutral atoms or molecules, the particle at certain incident conditions can orbit around the scattering center. This trapping phenomenon is known as “orbiting” [48], and can be predicted from the interaction potential between them.

The Lennard-Jones potential is a simple mathematical model for a part of this interaction, which is of the form:

$$V(r) = 4\epsilon \left[ \left( \frac{\sigma}{r} \right)^{12} - \left( \frac{\sigma}{r} \right)^6 \right], \quad (4.1.1)$$

where  $r$  is the distance between particles. The constants  $\epsilon$  and  $\sigma$  are the depth of the

potential well and the distance at which the inter-particle potential is zero, respectively. The other part is the centrifugal potential associated with the angular motion of the incident particle around the scattering center. Thus, the effective potential describing the interaction between them, a pair of neutral atoms or molecules, is given by

$$V_{eff}(r) = V(r) + \frac{l^2}{2\mu r^2}, \quad (4.1.2)$$

where  $l$  is the angular momentum, and  $\mu$  is the reduced mass for the incident particle and the scattering center. Because the Lennard-Jones potential depends only on the distance between particles and not on the orientation, the angular momentum of this system is conserved. Thus, the effective potential Eq. (4.1.2) can be given by

$$V_{eff}(r) = V(r) + T_0 \left(\frac{b}{r}\right)^2, \quad (4.1.3)$$

where  $T_0$  is the energy of the incident particle, and  $b$  is the impact parameter - the perpendicular distance from the scattering center to the initial straight line of motion of the incident particle. This effective potential for various impact parameters with a given value of  $T_0$  is plotted in Figure 4.1 to graphically describe the effect of the centrifugal term.

The effective potential A is the Lennard-Jones potential with no centrifugal term, and allows bound states only if the energy is negative. For the effective potential B bound states can be formed not only when the energy is negative but also when the energy is zero or positive. For the effective potential C the centrifugal term dominates, and no bound state can exist. Thus, the bound states for the incident particle can be formed only for the effective potential B because the energy of the incident particle is positive.

If we assume that the change in the energy of the incident particle  $T_0$  would not alter the shape of the effective potential. (This can be achieved by adjusting the

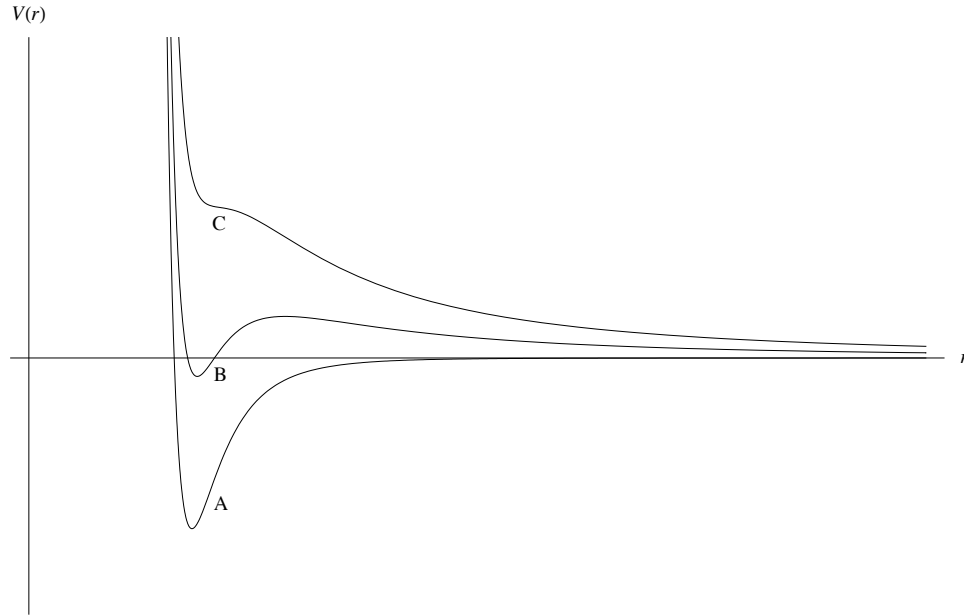


Fig 4.1. The effective potential for the interaction between a pair of neutral particles for various impact parameter values as a function of distance between the neutral particles. For the curve A bound states exist only if the energy is negative. For the curve B bound states exist even if the energy is positive. for the curve C no bound state exists.

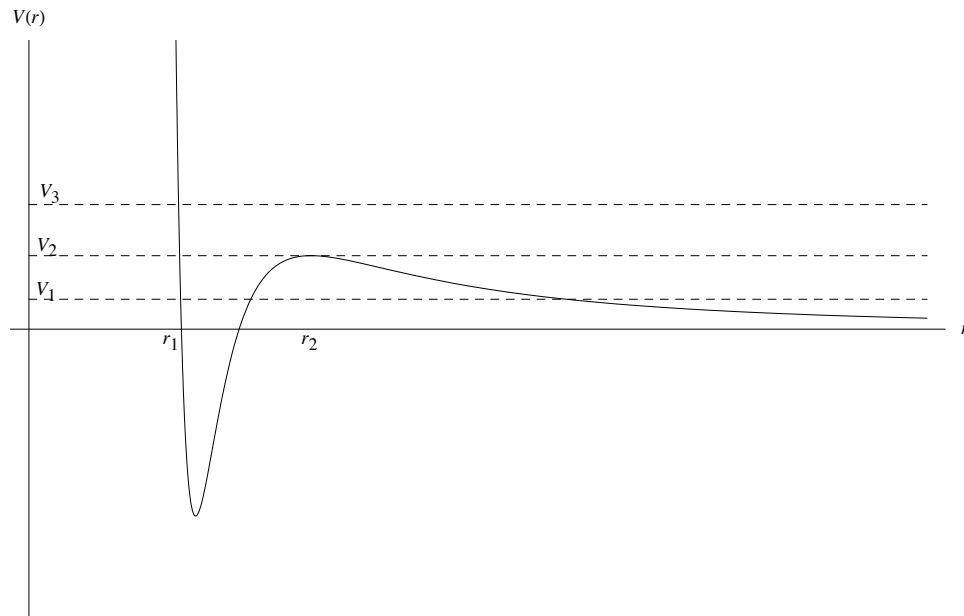


Fig 4.2. The effective potential B with various energies of the incident particle. If  $T_0 = V_1$  or  $T_0 = V_3$ , the incident particle cannot be bound. If  $T_0 = V_2$ , the particle can be bound in the region  $r_1 \leq r \leq r_2$ .

impact parameter value  $b$  as  $T_0$  changes.) Then, we can plot various energies of the incident particle  $T_0$  on the effective potential B as shown in Figure 4.2. If the energy

of the incident particle  $T_0$  is greater or less than energy  $V_2$ , such as  $V_1$  and  $V_3$  in Figure 4.2, then the particle cannot be bound: when the incident particle reaches the potential barrier, it is reflected back toward infinitely large  $r$ . However, if  $T_0 = V_2$ , then the incident particle passing through the point  $r_2$  can be bound in the region  $r_1 \leq r \leq r_2$ . This condition for orbiting occurs with only one impact parameter value for a given energy of the incident particle.

We now consider scattering of  $^1\text{H}_2$  from a carbon atom fixed at the origin to graphically describe orbiting. Because the effective potential, Eq. (4.1.3) is azimuthally symmetrical, the trajectory remains in one plane so it can be described in 2D. The Lennard-Jones potential parameters for the unlike particle interactions are usually estimated by the combining rules [49]:

$$\epsilon_{12} = \sqrt{\epsilon_{11} \epsilon_{22}}, \quad (4.1.4)$$

and

$$\sigma_{12} = \frac{1}{2}(\sigma_{11} + \sigma_{22}), \quad (4.1.5)$$

where  $\epsilon_{11}$  and  $\sigma_{11}$  ( $\epsilon_{22}$  and  $\sigma_{22}$ ) are the Lennard-Jones parameters for the like particle interactions. For the carbon - carbon interactions the parameters  $\epsilon_{\text{CC}}$  and  $\sigma_{\text{CC}}$  are 2.41 meV and 3.40 Å [27], and for the hydrogen - hydrogen interactions  $\epsilon_{\text{HH}}$  and  $\sigma_{\text{HH}}$  are 2.93 meV and 3.075 Å [50]. Therefore, using Eq. (4.1.4) and Eq. (4.1.5) the estimated Lennard-Jones potential parameters  $\epsilon_{\text{CH}}$  and  $\sigma_{\text{CH}}$  for the carbon - hydrogen interactions are 2.66 meV and 3.24 Å, respectively. Note that with these values the condition for orbiting is satisfied with only low energies of incident hydrogen molecules: If  $T_0 > 2.10$  meV, which corresponds to the energy of an ideal monoatomic gas at about 16 °K, no orbiting can occur.

The trajectory of the incident particle under the influence of the potential  $V(x, z)$  can be obtained by solving the second order differential equations:

$$\mu \ddot{x} = -\frac{\partial}{\partial x} V(x, z) \quad (4.1.6)$$

and

$$\mu\ddot{z} = -\frac{\partial}{\partial z}V(x, z), \quad (4.1.7)$$

where  $\mu$  is the reduced mass for  $\text{H}_2$  and C, and

$$V(x, z) = 4\epsilon_{\text{CH}} \left[ \frac{\sigma_{\text{CH}}^{12}}{(x^2 + z^2)^6} - \frac{\sigma_{\text{CH}}^6}{(x^2 + z^2)^3} \right]. \quad (4.1.8)$$

The initial velocity of the incident hydrogen molecule far away from the scattering center is taken to be in the  $x$ -direction only. The computed trajectories of the hydrogen molecule at different impact parameters with  $T_0 = 1.29$  meV are plotted in Figure 4.3. As shown, the incident hydrogen molecule with the impact parameter  $b = 6.25 \text{ \AA}$  is orbiting around the scattering center.

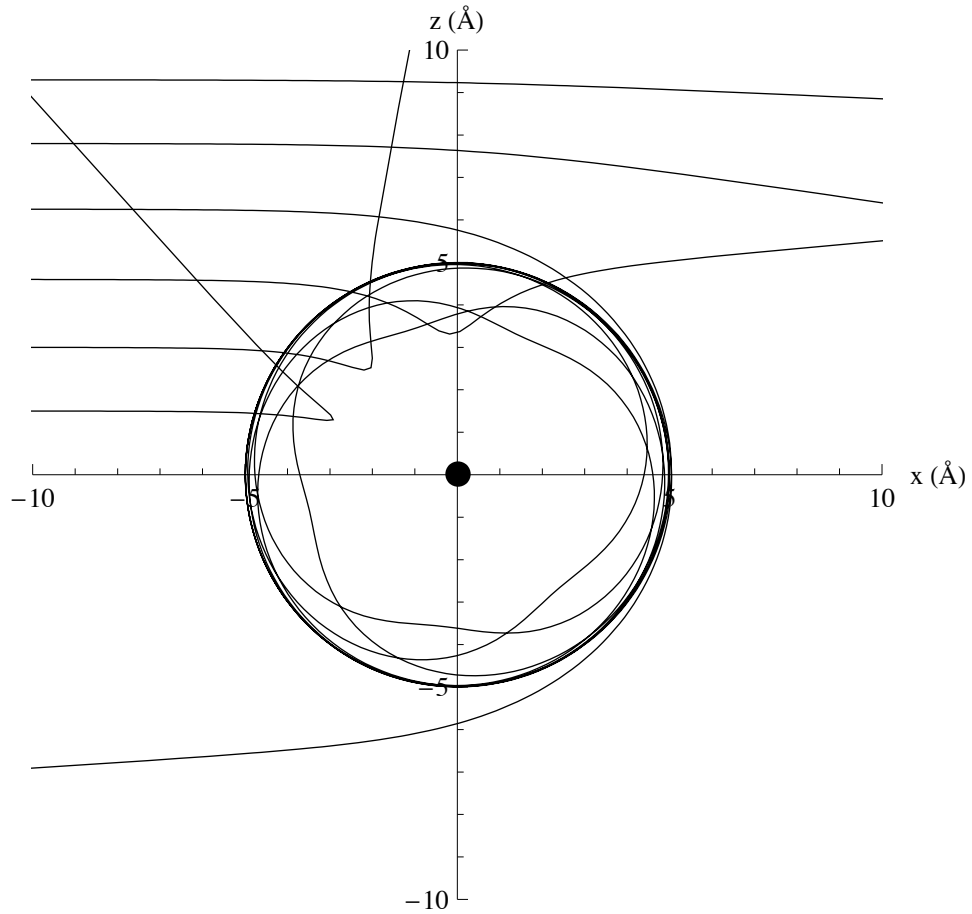


Fig 4.3. The trajectories of the incident hydrogen molecule at different impact parameters with  $T_0 = 1.29$  meV.

## 4.2 Periodic Scatterers

The interaction between an incident particle and periodic scatterers are sum of the interaction between an incident particle and each scatterer such that

$$V_M = 4\epsilon \sum_{i=0}^N \left[ \left( \frac{\sigma}{r - r_i} \right)^{12} - \left( \frac{\sigma}{r - r_i} \right)^6 \right], \quad (4.2.1)$$

where  $N$  is the number of scatterers and  $r_i$  is the location of each scatterer. Replacing the potentials in Eq. (4.1.6) and Eq. (4.1.7) with this potential, the trajectory of an incident particle involving multiple scatterers can be obtained.

We again use  $^1\text{H}_2$  for an incident particle and carbon atoms for scattering centers

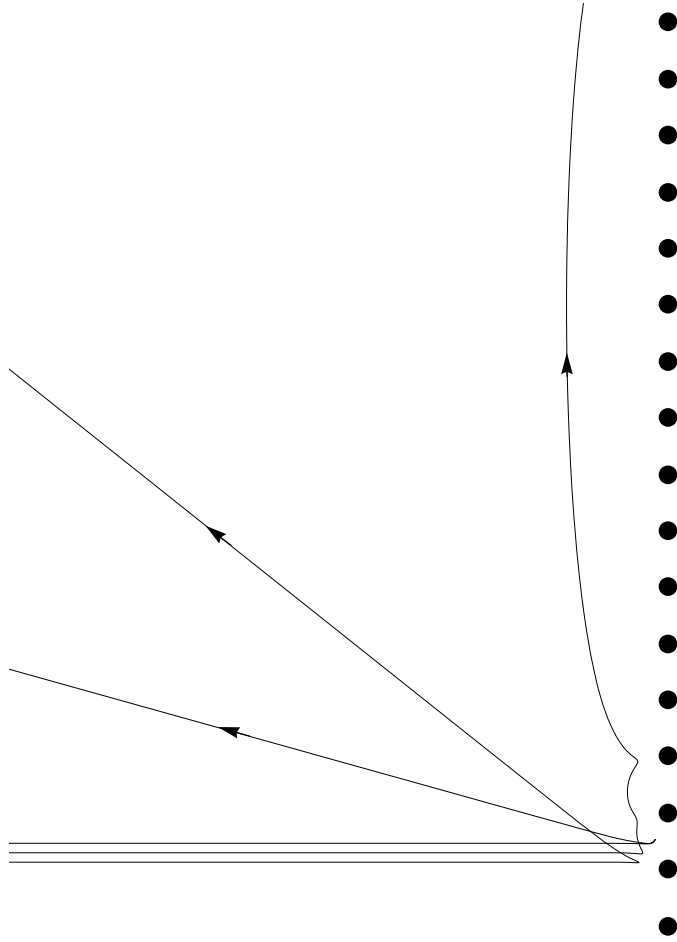


Fig 4.4. The trajectories of the incident hydrogen molecule in the one-dimensional lattice of carbon atoms at different impact parameters with  $T_0 = 1.29$  meV.



to graphically describe the trajectory of the incident particle. The distance between each carbon atom is arbitrarily chosen to be  $6.00 \text{ \AA}$ , and the initial velocity of the incident hydrogen molecule far away from the scattering centers is in the  $x$ -direction only with  $T_0 = 1.29 \text{ meV}$ . The trajectories with different impact parameters are shown in Figure 4.4.

For a special case as shown in Figure 4.4, when the incident hydrogen molecule comes close to the one-dimensional lattice of carbon atoms lying on the  $z$ -direction, a sufficient amount of its energy is transferred from the energy associated with motion in the  $x$ -direction to that in the  $z$ -direction during the initial collision, confining the incident hydrogen molecule near the one-dimensional lattice. This quasi-trapped case has been conjectured to be related to resonance scattering [47, 51], which is well understood in the quantum scattering theory. However, it cannot be classically treated with certainty because the trajectory is extremely sensitive to the initial conditions and even to round-off error in the computation.

CHAPTER 5  
QUANTUM SCATTERING IN 1D

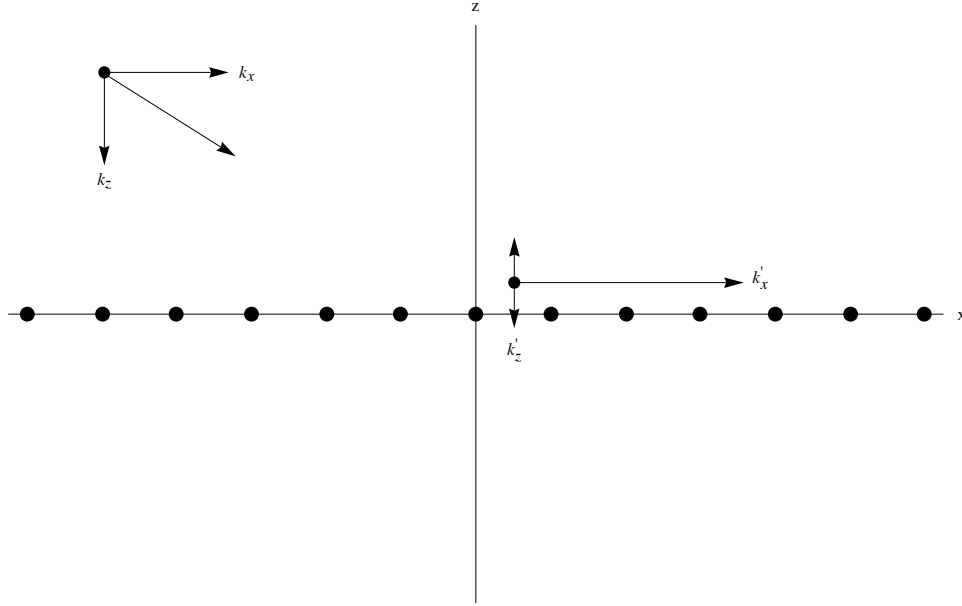


Fig 5.1. The two-dimensional system used in this thesis.  $k_x$  and  $k_z$  are the  $x$  and  $z$  components of the incident wave vector, and  $k'_x$  and  $k'_z$  are the  $x$  and  $z$  components of the diffracted wave vector.

For the two-dimensional system depicted in Figure 5.1 a bound state resonance can occur when the particle's energy associated with  $k'_z$  is equal to one of bound state energies of a laterally averaged potential  $w_0(z)$ , where  $k'_z$  is the  $z$  component of the diffracted wave vector. Thus, in order to obtain the condition for selective adsorption we need to acquire the expression for the bound state energy of the laterally averaged potential.

Because the laterally averaged potential depends only on  $z$ , the two-dimensional wave function can be expressed such that

$$\psi(x, z) = \phi(x)\phi(z). \quad (5.1)$$

Thus, we can study this system by a one-dimensional system first to obtain the properties of this one-dimensional system, such as bound state energies, transmission

and reflection amplitudes.

In section 3.4 the laterally averaged potential  $w_0(z)$  for the H<sub>2</sub>-graphite system was described. However, with that potential only a numerical solution for the Schrödinger equation can be obtained. Therefore, in this thesis we use a delta function potential as a laterally averaged potential because it allows us calculations and possesses properties of the realistic potential necessary for the study of the scattering process:

$$w_0(z) = -|g|\delta(z), \quad (5.2)$$

where  $g$  is a constant, which can be adjusted so that a bound state energy of this potential can be equal to one of bound state energies of the realistic potential. For an instance, with  $|g| = 13.11 \text{ meV}\cdot\text{Å}$  the delta function potential Eq. (5.2) can produce the ground state of the laterally averaged potential for the <sup>1</sup>H<sub>2</sub>-graphite system described in section 3.4.

### 5.1 Time Independent Wave Function

From Eq. (2.1.7) the one-dimensional Lippmann-Schwinger equation is given by

$$\psi(z) = \psi_0(z) + \frac{2m}{\hbar^2} \int dz' G(z, z') V(z') \psi(z'). \quad (5.1.1)$$

The plus sign (+) is omitted for brevity. With the delta function potential Eq. (5.2) it is given by

$$\psi(z) = \psi_0(z) + \frac{|g|}{2\pi} \int dz' \int dk' \frac{e^{ik'(z-z')}}{(\hbar k')^2/2m - E - i\epsilon} \delta(z') \psi(z'). \quad (5.1.2)$$

The integration over  $z$  results

$$\psi(z) = \psi_0(z) + \frac{|g|}{2\pi} \int dk' \frac{e^{ik'z}}{(\hbar k')^2/2m - E - i\epsilon} \psi(0). \quad (5.1.3)$$

The unknown  $\psi(0)$  can be removed from the integral sign since  $\psi(0)$  is independent of the integration variable  $k'$ . Thus, by setting  $z = 0$ , we obtain the self-consistency condition:

$$\left[1 - \frac{m|g|}{\pi\hbar^2} \int dk' \frac{1}{k'^2 - k^2 - i\epsilon'}\right] \psi(0) = \psi_0(0), \quad (5.1.4)$$

where  $k = \sqrt{2mE}/\hbar$ , and  $\epsilon' = 2m\epsilon/\hbar^2$ . The  $dk'$  integral in Eq. (5.1.4) is given by (Appendix B)

$$\int dk' \frac{1}{k'^2 - k^2 - i\epsilon'} = i\frac{\pi}{k}. \quad (5.1.5)$$

With this result Eq. (5.1.4) becomes

$$\left[1 - i\frac{m|g|}{\hbar^2 k}\right] \psi(0) = \psi_0(0). \quad (5.1.6)$$

The expressions in the square bracket cannot be zero so  $\psi(0)$  can be given by

$$\psi(0) = \frac{\hbar^2 k}{\hbar^2 k - im|g|} \psi_0(0). \quad (5.1.7)$$

Replacing  $\psi(0)$  in Eq. (5.1.3) with this result and using the free-particle Schrödinger equation approaching from  $+\infty$  for  $\psi_0(z)$ , the wave function  $\psi(z)$  becomes

$$\psi(z) = e^{-ikz} + \frac{m|g|k}{\pi(\hbar^2 k - im|g|)} \int dk' \frac{e^{ik'z}}{k'^2 - k^2 - i\epsilon'}. \quad (5.1.8)$$

The denominator in the integrand in Eq. (5.1.8) is identical to that in Eq. (5.1.5), so the poles occur at the same points. However, it requires a great caution to choose either the upper or lower half-plane because of the exponential  $e^{ik'z}$  in the numerator. For the case  $z > 0$ , the exponential increases without limit in the lower half-plane. Thus, the upper half-plane must be used to close the contour. The contour integral over  $dk'$  closed at infinity with a semicircle in the upper half-plane is given by

$$\int dk' \frac{e^{ik'z}}{k'^2 - k^2 - i\epsilon'} = \pi i \frac{e^{ikz}}{k}. \quad (5.1.9)$$

For  $z < 0$ , the lower half-plane must be used to close the contour. The contour integral over  $dk'$  closed at infinity with a semicircle in the lower half-plane is given by

$$\int dk' \frac{e^{ik'z}}{k'^2 - k^2 - i\epsilon'} = \pi i \frac{e^{-ikz}}{k}. \quad (5.1.10)$$

Combining Eq. (5.1.9) and Eq. (5.1.10), the integral over  $dk'$  is given by

$$\int dk' \frac{e^{ik'z}}{k'^2 - k^2 - i\epsilon'} = \pi i \frac{e^{ik|z|}}{k}. \quad (5.1.11)$$

Thus, the wave function  $\psi(z)$  is given by

$$\psi(z) = e^{-ikz} + \frac{im|g|}{\hbar^2 k - im|g|} e^{ik|z|}. \quad (5.1.12)$$

From this wave function the transmission and reflection amplitudes,  $T(k)$  and  $R(k)$  can be easily obtained: For  $z > 0$  the wave function is the combination of an incident wave and a reflected wave, and for  $z < 0$  it is just a transmitted wave. Thus, the expressions for  $T(k)$  and  $R(k)$  extracted from the wave function are

$$T(k) = \frac{\hbar^2 k}{\hbar^2 k - im|g|}, \quad (5.1.13)$$

and

$$R(k) = \frac{im|g|}{\hbar^2 k - im|g|}. \quad (5.1.14)$$

So far, we implicitly assume  $E > 0$  because if  $E < 0$ ,  $\psi_0(z)$  in Eq. (5.1.1) grow exponentially without limit as  $z$  approaches either  $+\infty$  or  $-\infty$ , depending on the initial direction the particle travels. Thus, if  $E < 0$ ,  $\psi_0(z)$  in Eq. (5.1.1) is not allowable. That is, the wave function is given by

$$\psi(z) = \frac{2m}{\hbar^2} \int dz' G(z, z') V(z') \psi(z'). \quad (5.1.15)$$

If we define  $k \equiv i\kappa$ , where  $\kappa$  is a real number, the negative energy can be expressed as

$$E = -\frac{\hbar^2 \kappa^2}{2m}. \quad (5.1.16)$$

Then, the wave function for the delta function potential Eq. (5.2) after integrating over  $z'$  can be given by

$$\psi(z) = \frac{m|g|}{\pi\hbar^2} \int dk' \frac{e^{ik'z}}{k'^2 + \kappa^2 - i\epsilon} \psi(0). \quad (5.1.17)$$

The integration over  $dk'$  is obtained by the same procedure as followed to obtain Eq. (5.1.11), and the result is given by

$$\int dk' \frac{e^{ik'z}}{k'^2 + \kappa^2 - i\epsilon} = \pi \frac{e^{-\kappa|z|}}{\kappa}. \quad (5.1.18)$$

Thus, the wave function, when  $E < 0$ , is given by

$$\psi(z) = \frac{m|g|}{\hbar^2\kappa} e^{-\kappa|z|} \psi(0). \quad (5.1.19)$$

This wave function approaches zero as  $|z|$  increases, which is a main property of bound-state wave functions. If we set  $z = 0$ , then from the self-consistency condition we obtain a possible value for  $\kappa$ :

$$\kappa = \frac{m|g|}{\hbar^2}. \quad (5.1.20)$$

Thus, the bound state energy is given by

$$E_{bound} = -\frac{mg^2}{2\hbar^2}. \quad (5.1.21)$$

Note that the delta function potential Eq. (5.2) has one and only one bound state with any given value of  $g$ .

The normalized bound-state wave function can be obtained by solving the differential form of the Schrödinger equation, which is given by (Appendix C)

$$\psi(z) = \pm \frac{\sqrt{m|g|}}{\hbar} e^{-m|g||z|/\hbar^2}. \quad (5.1.22)$$

## 5.2 Time Dependent Wave Function

In section 2.3 we showed that a particle with a definite momentum is un-physical, and the wave packet, a spread of momenta, should be used for the time-dependent solution. Here we construct a one-dimensional Gaussian wave packet with the obtained time-independent wave function Eq. (5.1.12) such that

$$\Psi(z, t) = \int_{-\infty}^{\infty} dk e^{-(k-k_0)^2/2\sigma_k^2} \left[ e^{-ikz} + \frac{im|g|}{\hbar^2 k - im|g|} e^{ik|z|} \right] e^{-i\hbar k^2 t/2m}. \quad (5.2.1)$$

We first treat the integral with the first term in the square bracket  $\Psi_0(z, t)$ , which is merely the wave packet for free particles. If we define  $\rho \equiv (k - k_0) / \sqrt{2}\sigma_k$ , then it can be given by

$$\Psi_0(z, t) = \int_{-\infty}^{\infty} \sqrt{2}\sigma_k d\rho e^{-\rho^2} e^{-i(\sqrt{2}\sigma_k \rho + k_0)z} e^{-i\hbar(\sqrt{2}\sigma_k \rho + k_0)^2 t/2m}. \quad (5.2.2)$$

Rearranging the exponents in terms of  $\rho$  and defining  $\xi \equiv \rho\sqrt{1 + i\sigma_k^2 \hbar t/m}$ , Eq. (5.2.2) can be given by

$$\begin{aligned} \Psi_0(z, t) &= \sqrt{2}\sigma_k \exp \left[ -i(k_0 z + \frac{\hbar k_0^2 t}{2m}) \right] \frac{1}{\sqrt{1 + i\sigma_k^2 \hbar t/m}} \\ &\times \int_{-\infty}^{\infty} d\xi \exp \left[ -\xi^2 - \frac{i\sqrt{2}\sigma_k(z + \hbar k_0 t/m)}{\sqrt{1 + i\sigma_k^2 \hbar t/m}} \xi \right]. \end{aligned} \quad (5.2.3)$$

If we define the coefficient of  $\xi$  in the exponent as  $\alpha$  and complete the square, then Eq. (5.2.3) can be given by

$$\Psi_0(z, t) = \frac{\sqrt{2}\sigma_k \exp[-i(k_0 z + \hbar k_0^2 t/2m)] \exp[\alpha^2/4]}{\sqrt{1 + i\sigma_k^2 \hbar t/m}} \int_{-\infty}^{\infty} d\eta e^{-\eta^2}, \quad (5.2.4)$$

where  $\eta \equiv \xi + \alpha/2$ . The definite integral in this equation is the well-known Gaussian integral and has the value of  $\sqrt{\pi}$ . Thus, the wave packet for free particles is given by

$$\Psi_0(z, t) = \frac{\sqrt{2\pi}\sigma_k}{\sqrt{1 + i\sigma_k^2 \hbar t/m}} \exp[-i(k_0 z + \omega_0 t)] \exp \left[ -\frac{\sigma_k^2(z + v_0 t)^2}{2(1 + i\sigma_k^2 \hbar t/m)} \right], \quad (5.2.5)$$

where  $\omega_0 = \hbar k_0^2/2m$  and  $v_0 = \hbar k_0/m$ .

The obtained wave function is in the coordinate space so it would be better to use the width of the wave packet in the coordinate space  $\sigma_z$  instead of that in the  $k$  space  $\sigma_k$ . According to the uncertainty principle, the relationship between  $\sigma_z$  and  $\sigma_k$  is given by

$$\sigma_z = \frac{1}{\sigma_k}. \quad (5.2.6)$$

With this relation, the wave packet for free particles is given by

$$\Psi_0(z, t) = \frac{\sqrt{2\pi}}{\sigma_z \sqrt{1 + it/\tau}} \exp[-i(k_0 z + \omega_0 t)] \exp\left[-\frac{(z + v_0 t)^2}{2\sigma_z^2(1 + it/\tau)}\right], \quad (5.2.7)$$

where  $\tau = m\sigma_z^2/\hbar$ .

The procedures for the integral with the second term in the square bracket  $\Psi_s$  is identical to the first one. After following the same procedures, the scattered part of the Gaussian wave packet is given by

$$\Psi_s(z, t) = A \int_{-\infty}^{\infty} d\eta \frac{e^{-\eta^2}}{\eta + \gamma(z, t)}, \quad (5.2.8)$$

where

$$A = \frac{im|g|}{\hbar^2} \exp[i(k_0|z| - \omega_0 t)] \exp\left[-\frac{(|z| - v_0 t)^2}{2\sigma_z^2(1 + it/\tau)}\right], \quad (5.2.9)$$

$$\gamma(z, t) = \frac{1}{\sqrt{2}} \left[ \frac{i(|z| - v_0 t)}{\sigma_z \sqrt{1 + it/\tau}} + \left( k_0 - \frac{im|g|}{\hbar^2} \right) \sigma_z \sqrt{1 + it/\tau} \right]. \quad (5.2.10)$$

The integral in Eq. (5.2.8), if  $\text{Im}[\gamma(\alpha', \beta)] \neq 0$ , is given by [52]

$$\int_{-\infty}^{\infty} d\eta \frac{e^{-\eta^2}}{\eta + \gamma} = \gamma \sqrt{-\frac{1}{\gamma^2}} e^{-\gamma^2} \pi \left[ -2 + \text{erfc} \left( \gamma^2 \sqrt{-\frac{1}{\gamma^2}} \right) \right], \quad (5.2.11)$$

where  $\text{erfc}(z)$  is the complementary error function. This form of the solution is not



stable when the modulus of  $\gamma$  is large because the exponent becomes very large while the complementary error function becomes very small. Thus, we rewrite the terms in the bracket to resolve this problem using the properties of the error function:

$$\operatorname{erfc}(z) = 1 - \operatorname{erf}(z), \quad (5.2.12)$$

$$\operatorname{erf}(-z) = -\operatorname{erf}(z). \quad (5.2.13)$$

The result is given by

$$\int_{-\infty}^{\infty} d\eta \frac{e^{-\eta^2}}{\eta + \gamma} = -\gamma \sqrt{-\frac{1}{\gamma^2}} e^{-\gamma^2} \pi \operatorname{erfc} \left( -\gamma^2 \sqrt{-\frac{1}{\gamma^2}} \right). \quad (5.2.14)$$

This form of the solution does not have the problem when the modulus of  $\gamma$  is large because the solution of this integral becomes

$$\int_{-\infty}^{\infty} d\eta \frac{e^{-\eta^2}}{\eta + \gamma} \approx \frac{\sqrt{\pi}}{\gamma} \left[ 1 + \sum_{n=1}^{\infty} (-1)^n \frac{1 \cdot 3 \dots (2n-1)}{(-2\gamma^2)^n} \right] \quad (5.2.15)$$

with the asymptotic expansion of  $\operatorname{erfc}(z)$ , which is given by

$$\operatorname{erfc}(z) \approx \frac{e^{-z^2}}{z\sqrt{\pi}} \left[ 1 + \sum_{n=1}^{\infty} (-1)^n \frac{1 \cdot 3 \dots (2n-1)}{(2z^2)^n} \right]. \quad (5.2.16)$$

The scattered part of the Gaussian wave packet is thus given by

$$\begin{aligned} \Psi_s(z, t) = & -\frac{im|g|}{\hbar^2} \exp[i(k_0|z| - \omega_0 t)] \exp \left[ -\frac{(|z| - v_0 t)^2}{2\sigma_z^2(1 + it/\tau)} \right] \\ & \times \gamma(z, t) \sqrt{-\frac{1}{\gamma(z, t)^2}} e^{-\gamma(z, t)^2} \pi \operatorname{erfc} \left[ -\gamma(z, t)^2 \sqrt{-\frac{1}{\gamma(z, t)^2}} \right]. \end{aligned} \quad (5.2.17)$$

Finally, the Gaussian wave packet for the obtained time-independent wave function is given by

$$\begin{aligned}
\Psi(z, t) &= \Psi_0(z, t) + \Psi_s(z, t) \\
&= \frac{\sqrt{2\pi}}{\sigma_z \sqrt{1 + it/\tau}} \exp[-i(k_0 z + \omega_0 t)] \exp\left[-\frac{(z + v_0 t)^2}{2\sigma_z^2(1 + it/\tau)}\right] \\
&\quad - \frac{im|g|}{\hbar^2} \pi \exp[i(k_0 |z| - \omega_0 t)] \exp\left[-\frac{(|z| - v_0 t)^2}{2\sigma_z^2(1 + it/\tau)}\right] \\
&\quad \times \gamma(z, t) \sqrt{-\frac{1}{\gamma(z, t)^2}} e^{-\gamma(z, t)^2} \operatorname{erfc}\left[-\gamma(z, t)^2 \sqrt{-\frac{1}{\gamma(z, t)^2}}\right]. \tag{5.2.18}
\end{aligned}$$

The total probability density for finding the wave packet at time  $t$  is unity. In other words, the integral of  $|\Psi|^2$  must be unity if  $\Psi$  is normalized:

$$\int_{-\infty}^{\infty} |\Psi(z, t)|^2 dz = 1. \tag{5.2.19}$$

Thus, the square modulus integral of Eq. (5.2.18) with the proper normalization factor should yield unity. However, we cannot obtain its solution in an analytic form. Instead, if considering a wave packet very far from the scattering center, we can safely drop the second term  $\Psi_s$  in Eq. (5.2.18), and obtain the proper normalization factor  $N$  just from the square modulus integral of the first term  $\Psi_0$  because of the conservation of the total probability density. That is,

$$N^2 \frac{2\pi}{\sigma_z^2 \sqrt{1 + t^2/\tau^2}} \int_{-\infty}^{\infty} dz \exp\left[-\frac{(z + v_0 t)^2}{\sigma_z^2(1 + t^2/\tau^2)}\right] = 1. \tag{5.2.20}$$

Thus, the normalization factor  $N$  is given by

$$N = \sqrt{\frac{\sigma_z}{2\pi}} \left(\frac{1}{\pi}\right)^{1/4}. \tag{5.2.21}$$

Attaching this normalization factor to Eq. (5.2.18), we finally obtain the normalized Gaussian wave packet for the delta function potential Eq. (5.2):

$$\begin{aligned}
\Psi(z, t) = & \sqrt{\frac{\sigma_z}{2}} \left(\frac{1}{\pi}\right)^{1/4} \left\{ \frac{\sqrt{2}}{\sigma_z \sqrt{1 + it/\tau}} \exp[-i(k_0 z + \omega_0 t)] \exp\left[-\frac{(z + v_0 t)^2}{2\sigma_z^2(1 + it/\tau)}\right] \right. \\
& - i \frac{m|g|}{\hbar^2} \sqrt{\pi} \exp[i(k_0 |z| - \omega_0 t)] \exp\left[-\frac{(|z| - v_0 t)^2}{2\sigma_z^2(1 + it/\tau)}\right] \\
& \left. \times \gamma(z, t) \sqrt{-\frac{1}{\gamma(z, t)^2}} e^{-\gamma(z, t)^2} \operatorname{erfc}\left[-\gamma(z, t)^2 \sqrt{-\frac{1}{\gamma(z, t)^2}}\right] \right\}. \quad (5.2.22)
\end{aligned}$$

### 5.3 Graphical Description of Wave Packet

The Gaussian wave packet spreads out as it propagates. This dispersion should be minimized to obtain better graphical description of the interaction. In order to learn how fast the wave packet disperses the square modulus of the wave packet for a free particle is calculated such that

$$|\Psi_0(z, t)|^2 = \left(\frac{1}{\pi}\right)^{1/2} \frac{1}{\sigma_z \sqrt{1 + t^2/\tau^2}} \exp\left[-\frac{(z + v_0 t)^2}{\sigma_z^2(1 + t^2/\tau^2)}\right]. \quad (5.3.1)$$

From Equation (5.3.1), the time dependence of the width of the wave packet can be easily obtained, which is given by

$$\sigma_z(t) = \sigma_z(0) \sqrt{1 + \frac{t^2}{\tau^2}}, \quad (5.3.2)$$

where  $\sigma_z(0)$  is the initial width of the wave packet at  $t = 0$ . Note that as the wave packet's width disperses, its amplitude decreases, making the probability density of the wave packet intact.

For  $^1\text{H}_2$  at the temperature of 10 °K, it takes about 24 ps to travel 200 Å. In order to find the optimum initial width  $\sigma_z(0)$  for this distance, which minimizes the dispersion and also has the relatively small initial width of the wave packet, Eq. (5.3.2) with different  $\sigma_z(0)$  is plotted in Figure 5.2. As shown,  $\sigma_z(t)$  changes very slightly when the initial width is in the range between 20 Å and 25 Å so any value

in this range can be used. However,  $20 \text{ \AA}$  is the smallest initial width in this range. Thus, this value will be used in graphical description of the Gaussian wave packet throughout this thesis.

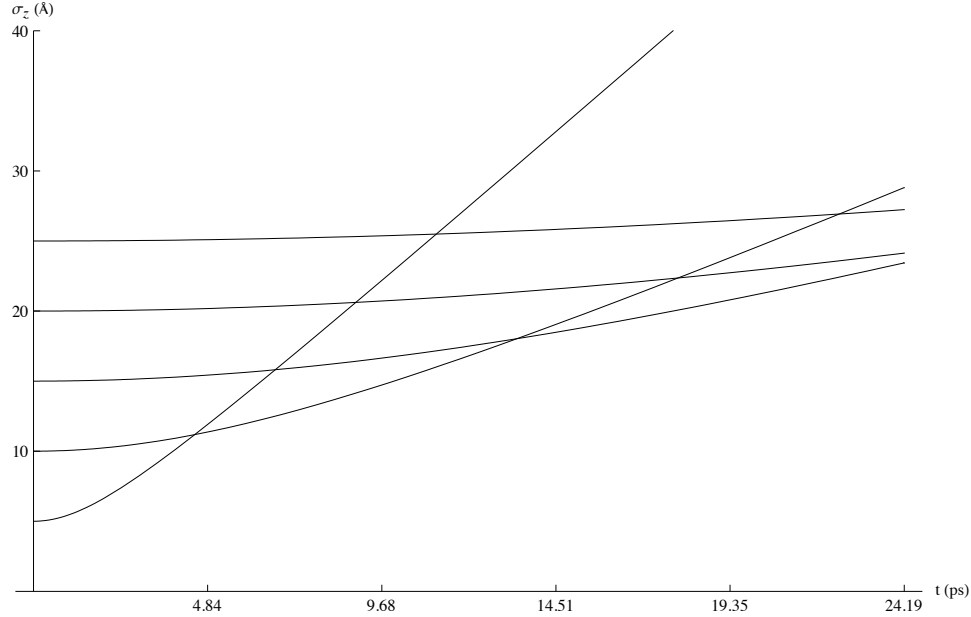


Fig 5.2. The time dependence of the width of the Gaussian wave packet.

With the initial width of  $20 \text{ \AA}$ , the Gaussian wave packets of  $^1\text{H}_2$  at the temperature of  $10 \text{ }^\circ\text{K}$  with different values of  $|g|$  are plotted to graphically describe the time evolution of the scattering process. In Figure 5.3 the Gaussian wave packets with  $|g| = 0.144 \text{ meV}\cdot\text{\AA}$  are plotted at different times. As shown, the wave packet approaches the origin from the right and is distorted a little bit at the origin where the delta potential is located. Then, it proceeds to the left. In Figure 5.4 the Gaussian wave packets with  $|g| = 1.440 \text{ meV}\cdot\text{\AA}$  are shown. As it approaches to the origin, it is distorted and splits at the origin: about 70 % of the wave packet transmits and the rest reflects. In Figure 5.5 the Gaussian wave packets with  $|g| = 14.40 \text{ meV}\cdot\text{\AA}$  are plotted. The wave packet approaches to the origin and is severely distorted. Then, it turns back to the right. Note that for the last two cases the Gaussian wave packets reflect from the well, which cannot happen in classical theory.

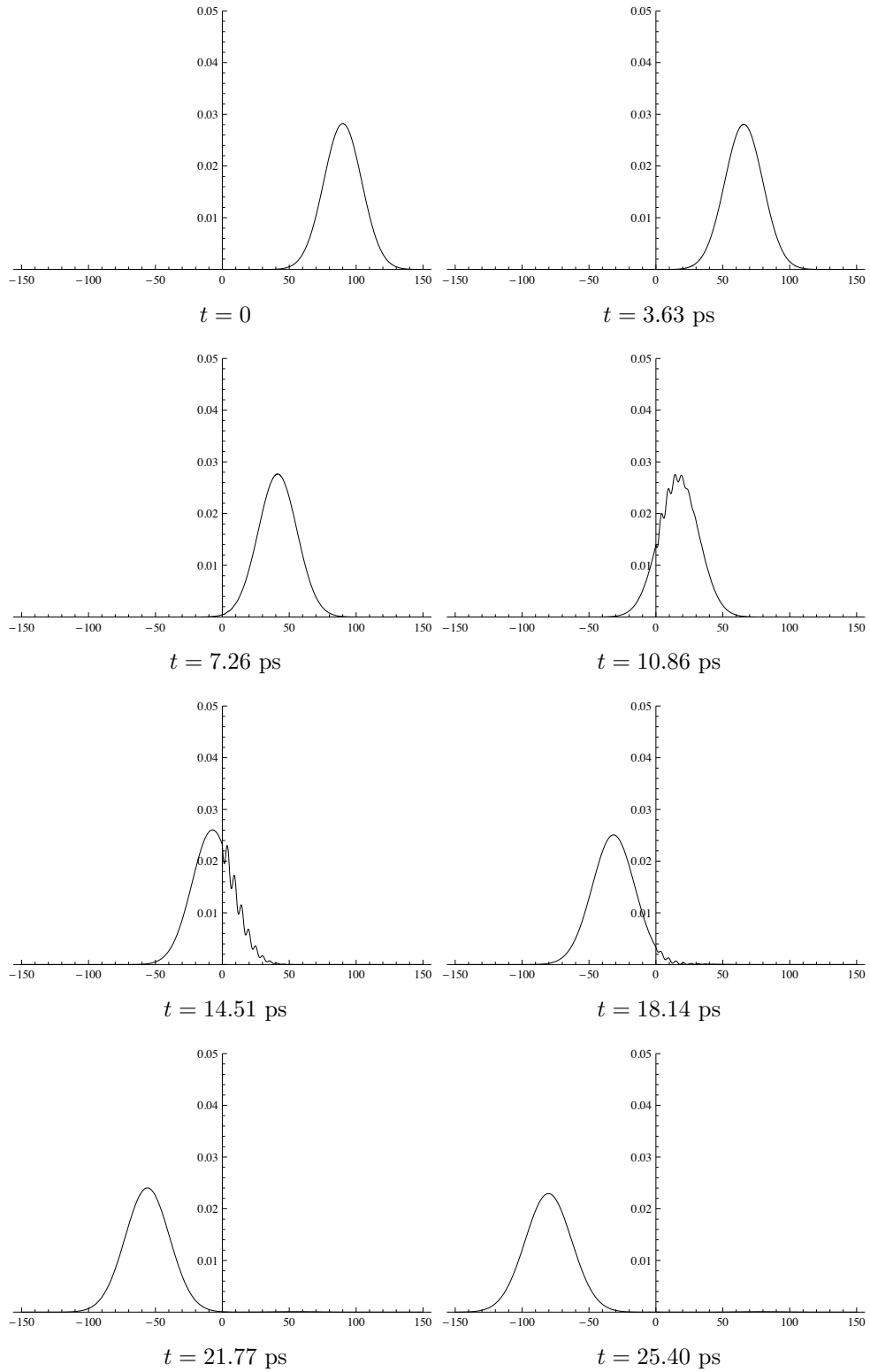


Fig 5.3. The Gaussian wave packet for  $^1\text{H}_2$  at the temperature of  $10^\circ\text{K}$  with  $|g| = 0.144 \text{ meV}\cdot\text{\AA}$  at different times.

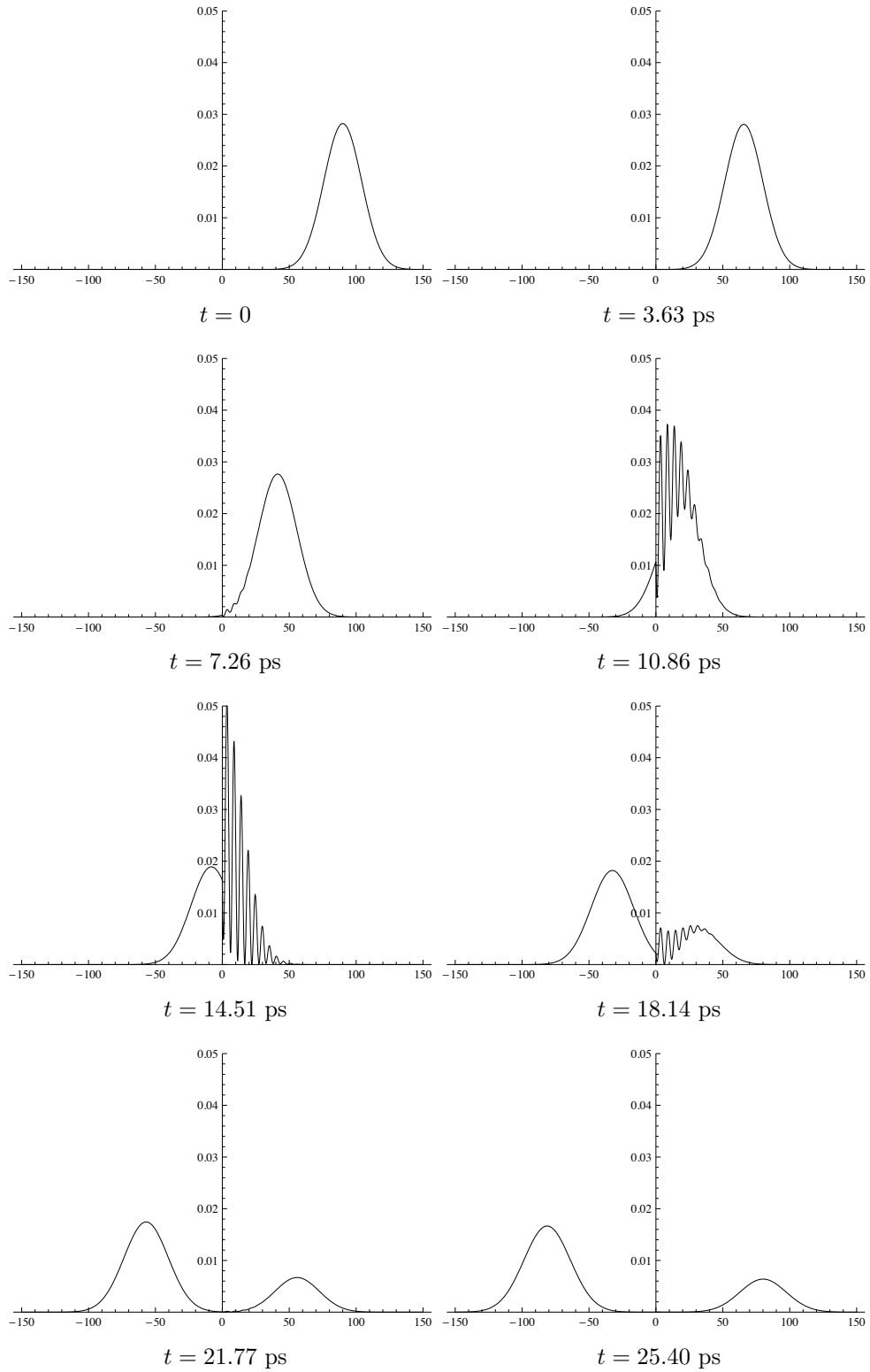


Fig 5.4. The Gaussian wave packet for  $^1\text{H}_2$  at the temperature of  $10^\circ\text{K}$  with  $|g| = 1.440 \text{ meV}\cdot\text{\AA}$  at different times.

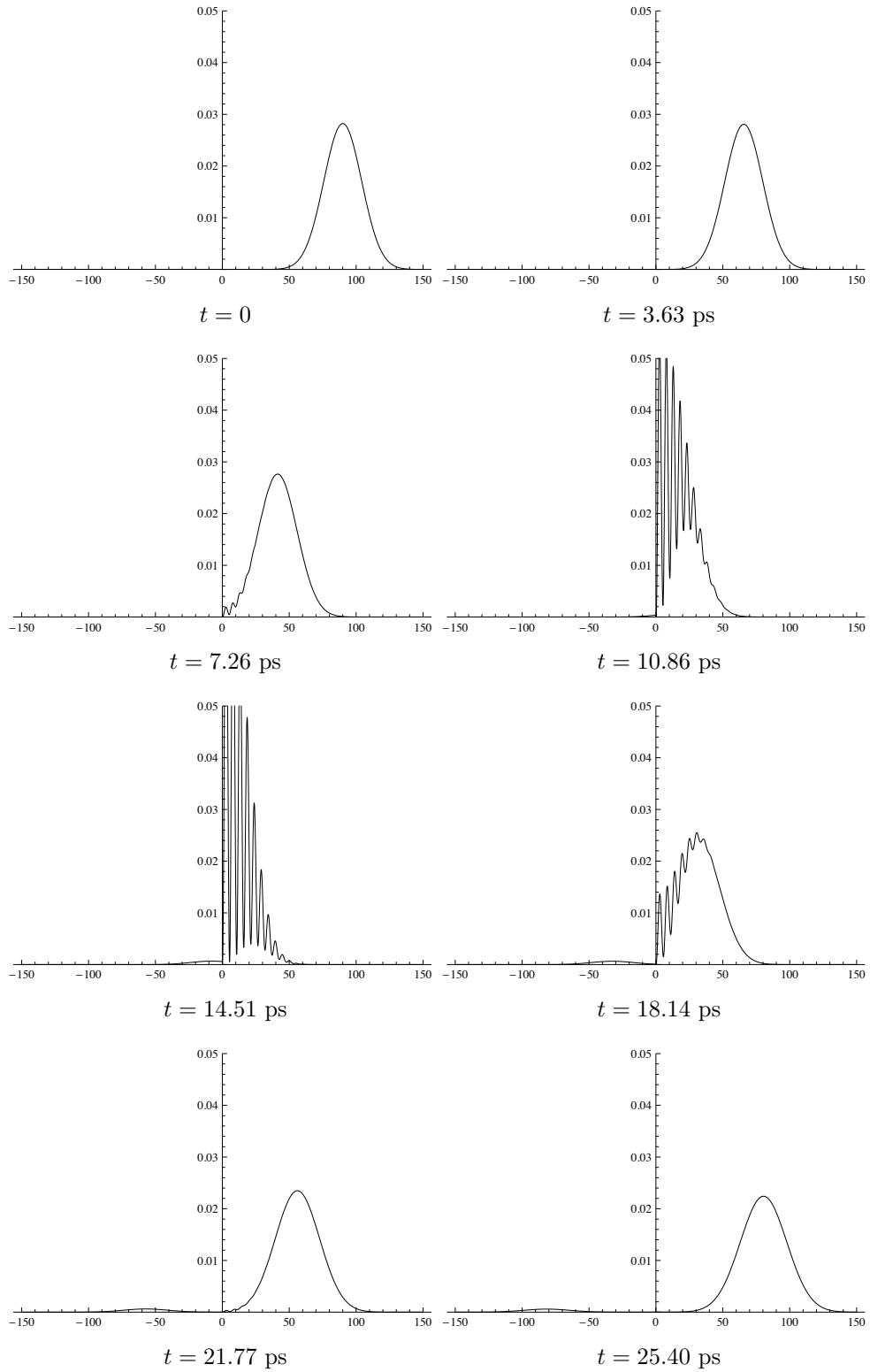


Fig 5.5. The Gaussian wave packet for  $^1\text{H}_2$  at the temperature of  $10^\circ\text{K}$  with  $|g| = 14.40 \text{ meV}\cdot\text{\AA}$  at different times.

In order to verify the results of graphical description, we numerically integrate the square modulus of the wave packet from  $-\infty$  to 0 to obtain the transmitted flux  $|T(k)|^2$  and from 0 to  $+\infty$  to obtain the reflected flux  $|R(k)|^2$  at  $t = 25$  ps, and compare to those computed by the square modulus of Eq. (5.1.13) and (5.1.14). The obtain values are reported in Table 2. As shown, their values are in excellent agreement, confirming the validity of graphical description.

Table 2

The transmitted and reflected fluxes  $|T(k)|^2$  and  $|R(k)|^2$  for  $^1\text{H}_2$  at 10 °K with different  $|g|$ .

$ g $ (meV·Å)	$ T(k) ^2$	$ R(k) ^2$
0.144	0.996 (0.996)	0.004 (0.004)
1.440	0.723 (0.724)	0.277 (0.276)
14.40	0.026 (0.026)	0.974 (0.974)

The transmitted and reflected fluxes are obtained first by integrating the square modulus of Eq. (5.2.22) from  $-\infty$  to 0 and from 0 to  $+\infty$  at  $t = 25$  ps, repectively, and then computed by the square modulus of Eq. (5.1.13) and (5.1.14). The values in the parenthesis are obtained by the latter.



## CHAPTER 6

### QUANTUM SCATTERING IN 2D

The two-dimensional version of the general periodic potential Eq. (3.1.6) for the system shown in Figure 5.1 is given by

$$V(x, z) = w_0(z) + 2 \sum_{G>0} w_G(z) \cos(Gx). \quad (6.1)$$

This potential can be further simplified by truncating higher terms because the value of  $w_G(z)$  for actual crystal potentials decrease rapidly as  $G$  increases [53]:

$$V(x, z) = w_0(z) + 2w_1(z) \cos\left(\frac{2\pi x}{a}\right), \quad (6.2)$$

where  $a$  is the distance between the interaction sites. From this simplified form we construct a model potential with the laterally averaged potential Eq. (5.2) used in the previous chapter such that

$$V(x, z) = -|g|\delta(z) + \lambda\delta(z) \cos\left(\frac{2\pi x}{a}\right), \quad (6.3)$$

where  $\lambda$  is a constant.

#### 6.1 Time Independent Wave Function

The two-dimensional Lippmann-Schwinger equation with the model potential Eq. (6.3) is given by

$$\begin{aligned} \psi(x, z) = & \psi_0(x, z) - \frac{|g|}{4\pi^2} \int dx' \int dz' \int dk_1 \int dk_2 \frac{e^{ik_1(x-x')} e^{ik_2(z-z')} \delta(z') \psi(x', z')}{E - \hbar^2(k_1^2 + k_2^2)/2m + i\epsilon} \\ & + \frac{\lambda}{4\pi^2} \int dx' \int dz' \int dk_1 \int dk_2 \frac{e^{ik_1(x-x')} e^{ik_2(z-z')} \delta(z') \cos(2\pi x'/a) \psi(x', z')}{E - \hbar^2(k_1^2 + k_2^2)/2m + i\epsilon}. \end{aligned} \quad (6.1.1)$$

Before proceeding with this equation, we first consider a limiting case  $\lambda = 0$ .

### 6.1.1 Non-periodic Potential

In this case we already know the solution from the fact that the solution of the two dimensional wave function if the potential depends only on one variable is the product of the one-dimensional wave functions of each variable. That is, with the time-independent wave function  $\psi(z)$  obtained in chapter 5, the solution for this non-periodic potential if the incident particle approaches from  $-\infty$  in the  $x$ -direction is given by

$$\psi(x, z) = e^{ik_x x} e^{-ik_z z} + \frac{im|g|}{\hbar^2 k_z - im|g|} e^{ik_x x} e^{ik_z |z|}. \quad (6.1.2)$$

However, it should be instructive to solve the same problem using another method, Fourier transform, that is not confined to single variable potentials. The equation that we need to solve is given by

$$\psi(x, z) = \psi_0(x, z) + \frac{|g|}{4\pi^2} \int dx' \int dk_1 \int dk_2 \int dz' \frac{e^{ik_1(x-x')} e^{ik_2(z-z')} \delta(z') \psi(x', z')}{\hbar^2(k_1^2 + k_2^2)/2m - E - i\epsilon}. \quad (6.1.3)$$

Integrating over  $z'$  results that

$$\psi(x, z) = \psi_0(x, z) + \frac{|g|}{4\pi^2} \int dx' \int dk_1 \int dk_2 \frac{e^{ik_1(x-x')} e^{ik_2 z} \psi(x', 0)}{\hbar^2(k_1^2 + k_2^2)/2m - E - i\epsilon}. \quad (6.1.4)$$

The equality of this equation should be satisfied with any value of  $z$ , so we can assign zero to  $z$  to make it independent of  $z$ . If we define  $f(x) \equiv \psi(x, 0)$ , then it can be given by

$$f(x) = f_0(x) + \frac{|g|}{4\pi^2} \int dx' \int dk_1 \int dk_2 \frac{e^{ik_1(x-x')} f(x')}{\hbar^2(k_1^2 + k_2^2)/2m - E - i\epsilon}. \quad (6.1.5)$$

In the Fourier Transform, a function of a real variable  $f(x)$  can be related to another function of another real variable  $F(k)$  such that

$$f(x) = \int dk e^{ikx} F(k) \quad \Longleftrightarrow \quad F(k) = \frac{1}{2\pi} \int dx e^{-ikx} f(x), \quad (6.1.6)$$

where  $F(k)$  is the Fourier transform of  $f(x)$  and  $f(x)$  is the inverse Fourier transform of  $F(k)$ . Fourier transforming Eq. (6.1.5), and integrating over  $x'$  and then over  $k_1$ , it becomes

$$\int d\kappa e^{i\kappa x} F(\kappa) = f_0(x) + \frac{|g|}{2\pi} \int dk_2 \int d\kappa \frac{e^{i\kappa x}}{\hbar^2(\kappa^2 + k_2^2)/2m - E - i\epsilon} F(\kappa). \quad (6.1.7)$$

Multiplying both sides by  $e^{-ikx}$  and integrating over  $x$  and then integrating over  $\kappa$ , Eq. (6.1.7) becomes

$$F(k) = \delta(k - k_x) + \frac{|g|}{2\pi} \int dk_2 \frac{F(k)}{\hbar^2(k^2 + k_2^2)/2m - E - i\epsilon}. \quad (6.1.8)$$

As before, if we use the free-particle approaching from  $-\infty$  for  $f_0(x)$  and combine  $F(k)$  terms together, Eq. (6.1.8) becomes

$$\left[ 1 - \frac{|g|}{2\pi} \int dk_2 \frac{1}{\hbar^2(k^2 + k_2^2)/2m - E - i\epsilon} \right] F(k) = \delta(k - k_x). \quad (6.1.9)$$

If  $k \neq k_x$ , then the left hand side of the equation should be zero for any  $k$ . Thus,  $F(k)$  must be zero. This is a trivial solution and doesn't give us any useful information. Therefore, we only consider the case  $k = k_x$  here. In this case, using the energy of the two dimensional free particle,

$$E = \frac{\hbar^2(k_x^2 + k_z^2)}{2m}, \quad (6.1.10)$$

Eq. (6.1.9) can be given by

$$\left[ 1 - \frac{m|g|}{\pi\hbar^2} \int dk_2 \frac{1}{k_2^2 - k_z^2 - i\epsilon'} \right] F(k) = \delta(k - k_x). \quad (6.1.11)$$

where  $\epsilon' = 2m\epsilon/\hbar^2$ . The integral over  $dk_2$  in this equation is obtained previously in chapter 5. With that result Eq. (6.1.11) is given by

$$\left[1 - \frac{im|g|}{\hbar^2 k_z}\right] F(k) = \delta(k - k_x). \quad (6.1.12)$$

Since the coefficient of  $F(k)$  cannot be zero,  $F(k)$  is given by

$$F(k) = \frac{\delta(k - k_x)}{1 - im|g|/\hbar^2 k_z}. \quad (6.1.13)$$

Transforming this  $F(k)$  back into  $f(x)$  using Eq. (6.1.6), we obtain

$$f(x) = \frac{e^{ik_x x}}{1 - im|g|/\hbar^2 k_z}. \quad (6.1.14)$$

Replacing  $\psi(x', 0)$  with this result, Eq. (6.1.4) is given by

$$\begin{aligned} \psi(x, z) &= \psi_0(x, z) + \frac{|g|}{4\pi^2} \int dx' \int dk_1 \\ &\times \int dk_2 \frac{e^{ik_1(x-x')} e^{ik_2 z}}{\hbar^2(k_1^2 + k_2^2)/2m - E - i\epsilon} \left( \frac{e^{ik_x x'}}{1 - im|g|/\hbar^2 k_z} \right). \end{aligned} \quad (6.1.15)$$

Integrating over  $x'$  followed by integrating over  $k_1$ , Eq. (6.1.15) becomes

$$\psi(x, z) = \psi_0(x, z) + \frac{m|g|}{\pi} \frac{k_z}{\hbar^2 k_z - im|g|} e^{ik_x x} \int dk_2 \frac{e^{ik_2 z}}{k_2^2 - k_z^2 - i\epsilon'}, \quad (6.1.16)$$

where  $\epsilon' = 2m\epsilon/\hbar^2$ . The integral in Eq. (6.1.16) is identical to Eq. (5.1.11) with  $k$  replaced by  $k_z$ . With that result, we finally obtain the non-trivial solution for the two dimensional wave function:

$$\psi(x, z) = e^{ik_x x} e^{-ik_z z} + \frac{im|g|}{\hbar^2 k_z - im|g|} e^{ik_x x} e^{ik_z |z|}, \quad (6.1.17)$$

where  $\psi_0(x, z)$  is replaced by the two-dimensional free particle Schrödinger equation which approaching from  $-\infty$  in the  $x$ -direction and from  $+\infty$  in the  $z$ -direction. As expected, this is identical to Eq. (6.1.2).

### 6.1.2 Periodic Potential

In the case  $\lambda \neq 0$  the potential depends on both variables  $x$  and  $z$ . Therefore, the method of separation of variables cannot be used. Here we use the method of Fourier transform used in the previous section to solve Eq. (6.1.1). As before, integrating over  $z'$ , assigning zero to  $z$  and defining  $f(x) \equiv \psi(x, 0)$ , Eq. (6.1.1) is given by

$$f(x) = f_0(x) + \frac{|g|}{4\pi^2} \int dx' \int dk_1 \int dk_2 \frac{e^{ik_1(x-x')}}{\hbar^2(k_1^2 + k_2^2)/2m - E - i\epsilon} f(x') \\ - \frac{\lambda}{4\pi^2} \int dx' \int dk_1 \int dk_2 \frac{e^{ik_1(x-x')}}{\hbar^2(k_1^2 + k_2^2)/2m - E - i\epsilon} \cos\left(\frac{2\pi x'}{a}\right) f(x'). \quad (6.1.18)$$

Fourier transforming this equation, multiplying both sides by  $e^{-ikx}$  and integrating over  $x$  and then over  $k_1$ , it becomes

$$F(k) = \delta(k - k_x) + \frac{|g|}{4\pi^2} \int dx' \int dk_2 \int d\kappa \frac{e^{i(\kappa-k)x'}}{\hbar^2(k^2 + k_2^2)/2m - E - i\epsilon} F(\kappa) \\ - \frac{\lambda}{4\pi^2} \int dx' \int dk_2 \int d\kappa \frac{e^{i(\kappa-k)x'}}{\hbar^2(k^2 + k_2^2)/2m - E - i\epsilon} \cos\left(\frac{2\pi x'}{a}\right) F(\kappa). \quad (6.1.19)$$

Replacing the cosine term using Euler's formula and integrating over  $x'$  and then over  $\kappa$ , Eq. (6.1.19) is given by

$$F(k) = \delta(k - k_x) + \frac{|g|}{2\pi} \int dk_2 \frac{1}{\hbar^2(k^2 + k_2^2)/2m - E - i\epsilon} F(k) \\ - \frac{\lambda}{4\pi} \int dk_2 \frac{F(k - 2\pi/a) + F(k + 2\pi/a)}{\hbar^2(k^2 + k_2^2)/2m - E - i\epsilon}. \quad (6.1.20)$$

Replacing  $E$  in terms of  $k_x$  and  $k_z$  and combining  $F(k)$  terms together, Eq. (6.1.20) becomes

$$\left(1 - \frac{m|g|}{\pi\hbar^2} \int dk_2 \frac{1}{k_2^2 - K - i\epsilon'}\right) F(k) = \delta(k - k_x) - \frac{m\lambda}{2\pi\hbar^2} \int dk_2 \frac{1}{k_2^2 - K - i\epsilon'} [F(k - 2\pi/a) + F(k + 2\pi/a)], \quad (6.1.21)$$

where  $K = k_x^2 + k_z^2 - k^2$ . The integrals over  $dk_2$  in this equation are obtained previously in chapter 5. With that result, Eq. (6.1.21) can be given by

$$\left(1 - \frac{im|g|}{\hbar^2 \sqrt{k_x^2 + k_z^2 - k^2}}\right) F(k) = \delta(k - k_x) - \frac{im\lambda}{2\hbar^2 \sqrt{k_x^2 + k_z^2 - k^2}} \left[F\left(k - \frac{2\pi}{a}\right) + F\left(k + \frac{2\pi}{a}\right)\right]. \quad (6.1.22)$$

Previously when  $\lambda = 0$ , we didn't worry about the coefficient of  $F(k)$  being zero: it cannot be zero when  $k = k_x$  and  $F(k)$  should be zero when  $k \neq k_x$ . However,  $F(k)$  in this equation is not necessarily zero when  $k \neq k_x$ . Thus, we should consider each case: the coefficient of  $F(k)$  is zero and not zero.

For the case in which the coefficient of  $F(k)$  is zero,  $k = \pm\sqrt{k_x^2 + k_z^2 + (m|g|)^2/\hbar^4}$ . Thus, Eq. (6.1.22) is given by

$$F\left(\pm\sqrt{k_x^2 + k_z^2 + \frac{(m|g|)^2}{\hbar^4}} - \frac{2\pi}{a}\right) = -F\left(\pm\sqrt{k_x^2 + k_z^2 + \frac{(m|g|)^2}{\hbar^4}} + \frac{2\pi}{a}\right). \quad (6.1.23)$$

This relation does not give us any useful information about  $F(k)$ . For the case that the coefficient of  $F(k)$  is not zero,  $F(k)$  can be given by

$$F(k) = \frac{\hbar^2 k_z}{\hbar^2 k_z - im|g|} \delta(k - k_x) - \frac{im\lambda}{2(\hbar^2 \sqrt{k_x^2 + k_z^2 - k^2} - im|g|)} \left[F\left(k - \frac{2\pi}{a}\right) + F\left(k + \frac{2\pi}{a}\right)\right]. \quad (6.1.24)$$

We cannot proceed any further with this equation because of the functions  $F(k - 2\pi/a)$

and  $F(k + 2\pi/a)$  on the right hand side of this equation. However, if we assume that  $\lambda$  is very small so that  $F(k)$  is not substantially altered by this  $\lambda$  term, we can well approximate  $F(k)$  using the Born approximation:

$$F_B(k) = \frac{\hbar^2 k_z}{\hbar^2 k_z - im|g|} \delta(k - k_x) - \frac{im\lambda}{2(\hbar^2 \sqrt{k_x^2 + k_z^2} - k^2 - im|g|)}$$

$$\times \left[ \frac{\hbar^2 k_z}{\hbar^2 k_z - im|g|} \delta(k - \frac{2\pi}{a} - k_x) + \frac{\hbar^2 k_z}{\hbar^2 k_z - im|g|} \delta(k + \frac{2\pi}{a} - k_x) \right]. \quad (6.1.25)$$

Transforming  $F_B(k)$  back into  $f_B(x)$ , Eq. (6.1.25) is given by

$$f_B(x) = \frac{\hbar^2 k_z}{\hbar^2 k_z - im|g|} \left\{ e^{ik_x x} - \frac{im\lambda}{2} \left[ \frac{e^{i(k_x + 2\pi/a)x}}{\hbar^2 \sqrt{k_z^2 - \frac{4\pi}{a}(k_x + \frac{\pi}{a})} - im|g|} \right. \right.$$

$$\left. \left. + \frac{e^{i(k_x - 2\pi/a)x}}{\hbar^2 \sqrt{k_z^2 + \frac{4\pi}{a}(k_x - \frac{\pi}{a})} - im|g|} \right] \right\}. \quad (6.1.26)$$

Replacing  $\psi(x', 0)$  with  $f_B(x)$  after integrating over  $z'$ , Eq. (6.1.1) is given by

$$\psi(x, z) = \psi_0(x, z) + \frac{|g|}{4\pi^2} \int dx' \int dk_1 \int dk_2 \frac{e^{ik_1(x-x')} e^{ik_2 z}}{\hbar^2(k_1^2 + k_2^2)/2m - E - i\epsilon} \frac{\hbar^2 k_z}{\hbar^2 k_z - im|g|}$$

$$\times \left\{ e^{ik_x x'} - \frac{im\lambda}{2} \left[ \frac{e^{i(k_x + 2\pi/a)x'}}{\hbar^2 \sqrt{k_z^2 - \frac{4\pi}{a}(k_x + \frac{\pi}{a})} - im|g|} + \frac{e^{i(k_x - 2\pi/a)x'}}{\hbar^2 \sqrt{k_z^2 + \frac{4\pi}{a}(k_x - \frac{\pi}{a})} - im|g|} \right] \right\}$$

$$- \frac{\lambda}{4\pi^2} \int dx' \int dk_1 \int dk_2 \frac{e^{ik_1(x-x')} e^{ik_2 z}}{\hbar^2(k_1^2 + k_2^2)/2m - E - i\epsilon} \frac{e^{i2\pi x'/a} + e^{-i2\pi x'/a}}{2} \frac{\hbar^2 k_z}{\hbar^2 k_z - im|g|}$$

$$\times \left\{ e^{ik_x x'} - \frac{im\lambda}{2} \left[ \frac{e^{i(k_x + 2\pi/a)x'}}{\hbar^2 \sqrt{k_z^2 - \frac{4\pi}{a}(k_x + \frac{\pi}{a})} - im|g|} + \frac{e^{i(k_x - 2\pi/a)x'}}{\hbar^2 \sqrt{k_z^2 + \frac{4\pi}{a}(k_x - \frac{\pi}{a})} - im|g|} \right] \right\}. \quad (6.1.27)$$

All integrals in this equation have the similar form and can be evaluated by the same procedure as before: First, integrate over  $x'$ , which yields a delta function and then integrate over  $k_1$ . Finally, integrate over  $k_z$ . The obtained wave function is given by

$$\begin{aligned}
\psi(x, z) = & e^{ik_x x} e^{-ik_z z} + \frac{im|g|}{\hbar^2 k_z - im|g|} e^{ik_x x} e^{ik_z |z|} - \frac{im\lambda\hbar^2 k_z}{2(\hbar^2 k_z - im|g|)} \\
& \times \left[ \frac{e^{i(k_x + \frac{2\pi}{a})x} e^{i\sqrt{k_z^2 - \frac{4\pi}{a}(k_x + \frac{\pi}{a})}|z|}}{\hbar^2 \sqrt{k_z^2 - \frac{4\pi}{a}(k_x + \frac{\pi}{a})} - im|g|} + \frac{e^{i(k_x - \frac{2\pi}{a})x} e^{i\sqrt{k_z^2 + \frac{4\pi}{a}(k_x - \frac{\pi}{a})}|z|}}{\hbar^2 \sqrt{k_z^2 + \frac{4\pi}{a}(k_x - \frac{\pi}{a})} - im|g|} \right] \\
& - \frac{\lambda^2}{4} \left\{ \frac{m^2 \hbar^2}{\hbar^2 k_z - im|g|} \left[ \frac{1}{\hbar^2 \sqrt{k_z^2 - \frac{4\pi}{a}(k_x + \frac{\pi}{a})} - im|g|} + \frac{1}{\hbar^2 \sqrt{k_z^2 + \frac{4\pi}{a}(k_x - \frac{\pi}{a})} - im|g|} \right] \right. \\
& \times e^{ik_x x} e^{ik_z |z|} + \frac{m^2 \hbar^2 k_z}{\hbar^2 k_z - im|g|} \left[ \frac{1}{\hbar^2 \sqrt{k_z^2 - \frac{8\pi}{a}(k_x + \frac{2\pi}{a})} - im|g|} \frac{e^{i(k_x + \frac{4\pi}{a})x} e^{i\sqrt{k_z^2 - \frac{8\pi}{a}(k_x + \frac{2\pi}{a})}|z|}}{\hbar^2 \sqrt{k_z^2 - \frac{4\pi}{a}(k_x + \frac{\pi}{a})} - im|g|} \right. \\
& \left. \left. + \frac{1}{\hbar^2 \sqrt{k_z^2 + \frac{8\pi}{a}(k_x - \frac{2\pi}{a})} - im|g|} \frac{e^{i(k_x - \frac{4\pi}{a})x} e^{i\sqrt{k_z^2 + \frac{8\pi}{a}(k_x - \frac{2\pi}{a})}|z|}}{\hbar^2 \sqrt{k_z^2 + \frac{4\pi}{a}(k_x - \frac{\pi}{a})} - im|g|} \right] \right\}. \tag{6.1.28}
\end{aligned}$$

In order to use the Born approximation we assumed that  $\lambda$  is very small, which allows us safely drop  $\lambda^2$  terms. Thus, the two-dimensional wave function can be given by

$$\psi(x, z) \approx e^{ik_x x} (e^{-ik_z z} + S_0 e^{ik_z |z|} + S_{-1} e^{ik_{-1,z} |z|} + S_{+1} e^{ik_{+1,z} |z|}), \tag{6.1.29}$$

where

$$S_0 = \frac{im|g|}{\hbar^2 k_z - im|g|}, \tag{6.1.30}$$

$$S_{-1} = -\frac{im\lambda}{2} \frac{\hbar^2 k_z}{(\hbar^2 k_z - im|g|)} \frac{e^{i2\pi x/a}}{(\hbar^2 k_{-1,z} - im|g|)}, \tag{6.1.31}$$



$$S_{+1} = -\frac{im\lambda}{2} \frac{\hbar^2 k_z}{(\hbar^2 k_z - im|g|)} \frac{e^{-i2\pi x/a}}{(\hbar^2 k_{+1,z} - im|g|)}, \quad (6.1.32)$$

and

$$k_{-1,z} = \sqrt{k_z^2 - \frac{4\pi}{a}(k_x + \frac{\pi}{a})}, \quad (6.1.33)$$

$$k_{+1,z} = \sqrt{k_z^2 + \frac{4\pi}{a}(k_x - \frac{\pi}{a})}. \quad (6.1.34)$$

As mentioned in chapter 5 selective adsorption for this system occurs when the particle's energy associated with the motion in the  $z$ -direction is equal to the bound state energy for  $w_0(z) = -|g|\delta(z)$ . That is, the particle can be selectively adsorbed when

$$k_{\pm 1,z} = i \frac{m|g|}{\hbar^2}. \quad (6.1.35)$$

Note these are poles of the wave function, which is a general property of scattering amplitudes: the appearance of a pole at a negative energy.

The kinematic condition of selective adsorption Eq. (6.1.35) in terms of the incident wave numbers can be given by

$$k_z^2 = -\frac{(m|g|)^2}{\hbar^4} \pm \frac{4\pi}{a} \left( k_x \pm \frac{n\pi}{a} \right). \quad (6.1.36)$$

If we add  $k_x^2$  to both sides and multiply both sides by  $\hbar^2/2m$ , this condition can be given by

$$E_i = E'_z + \frac{\hbar^2(k_x + G_{\pm 1})^2}{2m}, \quad (6.1.37)$$

where  $E_i$  is the initial energy of the incident particle,  $E'_z$  is the bound state energy and  $G_{\pm 1}$  is the reciprocal lattice vector in the  $x$ -direction. This expression indicates that motion of the selectively adsorbed particle parallel to the periodic potential site is restricted by the relation

$$k'_x = k_x + G_{\pm 1}, \quad (6.1.38)$$

where  $k'$  is the wave number of the selectively adsorbed particle in the  $x$ -direction. This is the well-known Laue condition. In other words, selective adsorption satisfies the diffraction condition.

## 6.2 Time Dependent Wave Function

As before we construct the Gaussian wave packet with the time-independent wave function obtained in the previous section such that

$$\begin{aligned} \Psi(x, z, t) = & \int_{-\infty}^{\infty} dk_x e^{(k_x - k_{x0})^2 / 2\sigma_{k_x}^2} \int_{-\infty}^{\infty} dk_z e^{(k_z - k_{z0})^2 / 2\sigma_{k_z}^2} \left\{ e^{ik_x x} e^{-ik_z z} \right. \\ & + \frac{im|g|}{\hbar^2 k_z - im|g|} e^{ik_x x} e^{ik_z |z|} - \frac{im\lambda}{2} \frac{\hbar^2 k_z}{\hbar^2 k_z - im|g|} \left[ \frac{e^{i(k_x + \frac{2\pi}{a})x} e^{i\sqrt{k_z^2 - \frac{4\pi}{a}(k_x + \frac{\pi}{a})}|z|}}{\hbar^2 \sqrt{k_z^2 - \frac{4\pi}{a}(k_x + \frac{\pi}{a})} - im|g|} \right. \\ & \left. \left. + \frac{e^{i(k_x - \frac{2\pi}{a})x} e^{i\sqrt{k_z^2 + \frac{4\pi}{a}(k_x - \frac{\pi}{a})}|z|}}{\hbar^2 \sqrt{k_z^2 + \frac{4\pi}{a}(k_x - \frac{\pi}{a})} - im|g|} \right] \right\} e^{-i\hbar k_x^2 t / 2m} e^{-i\hbar k_z^2 t / 2m}. \end{aligned} \quad (6.2.1)$$

The first and the second integrals are separable into  $k_x$  and  $k_z$  terms. The integrals with respect to  $k_z$  are treated and their analytic solutions are obtained in chapter 5, and the integral with respect to  $k_x$  is just a Gaussian wave packet for free particles approaching from  $-\infty$ . Thus, Eq. (6.2.1) can be given by

$$\Psi(x, z, t) = N \left[ \Psi_x^0(x, t) \Psi_z^0(z, t) + \Psi_x^0(x, t) \Psi_s(z, t) + \Psi_\lambda(x, z, t) \right], \quad (6.2.2)$$

where

$$\Psi_x^0(x, t) = \frac{\sqrt{2\pi}}{\sigma_x \sqrt{1 + it/\tau_x}} \exp [i(k_{x0}x - \omega_{x0}t)] \exp \left[ -\frac{(x - v_{x0}t)^2}{2\sigma_x^2(1 + it/\tau_x)} \right], \quad (6.2.3)$$

$$\Psi_z^0(z, t) = \frac{\sqrt{2\pi}}{\sigma_z \sqrt{1 + it/\tau_z}} \exp [-i(k_{z0}z + \omega_{z0}t)] \exp \left[ -\frac{(z + v_{z0}t)^2}{2\sigma_z^2(1 + it/\tau_z)} \right], \quad (6.2.4)$$

$$\begin{aligned} \Psi_s(z, t) &= -\frac{im|g|}{\hbar^2} \pi \exp [i(k_{z0}|z| - \omega_{z0}t)] \exp \left[ -\frac{(|z| - v_{z0}t)^2}{2\sigma_z^2(1 + it/\tau_z)} \right] \\ &\times \gamma(z, t) \sqrt{-\frac{1}{\gamma(z, t)^2}} e^{-\gamma(z, t)^2} \operatorname{erfc} \left[ -\gamma(z, t)^2 \sqrt{-\frac{1}{\gamma(z, t)^2}} \right], \end{aligned} \quad (6.2.5)$$

$$\begin{aligned} \Psi_\lambda(x, z, t) &= -\frac{im\lambda}{2} \int_{-\infty}^{\infty} dk_x \int_{-\infty}^{\infty} dk_z e^{(k_x - k_{x0})^2/2\sigma_{k_x}^2} e^{(k_z - k_{z0})^2/2\sigma_{k_z}^2} e^{-i\hbar k_x^2 t/2m} e^{-i\hbar k_z^2 t/2m} \\ &\times \frac{\hbar^2 k_z}{\hbar^2 k_z - im|g|} \left[ \frac{e^{i(k_x + \frac{2\pi}{a})x} e^{i\sqrt{k_z^2 - \frac{4\pi}{a}(k_x + \frac{\pi}{a})}|z|}}{\hbar^2 \sqrt{k_z^2 - \frac{4\pi}{a}(k_x + \frac{\pi}{a})} - im|g|} + \frac{e^{i(k_x - \frac{2\pi}{a})x} e^{i\sqrt{k_z^2 + \frac{4\pi}{a}(k_x - \frac{\pi}{a})}|z|}}{\hbar^2 \sqrt{k_z^2 + \frac{4\pi}{a}(k_x - \frac{\pi}{a})} - im|g|} \right], \end{aligned} \quad (6.2.6)$$

and  $N$  is a normalization factor.

As before, we consider the square modulus integral of the wave packet very far from the periodic interaction site to obtain the normalization factor. That is,

$$N^2 \int_{-\infty}^{\infty} dx \int_{-\infty}^{\infty} dz \Psi_x^0(x, t) \Psi_z^0(z, t) = 1. \quad (6.2.7)$$

The obtained normalization factor is given by

$$N = \frac{\sqrt{\sigma_x \sigma_z}}{2\pi^{3/2}}. \quad (6.2.8)$$

Thus, the two-dimensional normalized Gaussian wave packet can be given by

$$\Psi(x, z, t) = \frac{\sqrt{\sigma_x \sigma_z}}{2\pi^{3/2}} \left[ \Psi_x^0(x, t) \Psi_z^0(z, t) + \Psi_x^0(x, t) \Psi_s(z, t) + \Psi_\lambda(x, z, t) \right]. \quad (6.2.9)$$

The last term in the square bracket  $\Psi_\lambda(x, z, t)$  is in an integral form and can only be treated numerically. In general, for this type of integral whose integrand has highly oscillatory behavior, the accuracy of the result is limited even with special methods for this type of integrals, such as Levin method [54] and contour integration method. However, for the parameters used in this thesis, the result of this integral is

so small ( $|\Psi_\lambda(x, z, t)|^2 < 10^{-10}$ ) that it does not affect the probability density of the wave function, except when the integrand does not oscillate rapidly, where we can obtain a reliable result even with standard numerical methods, such as Simpson's rule. This integral also has another issue: two singular points in the integrand. However, the difference between the values calculated with and without consideration of those singularities is less than 1 % when the integrand does not oscillate rapidly. Therefore, in numerical calculation of the term  $\Psi_\lambda(x, z, t)$  Simpson's rule is used to minimize the computation time.

### 6.3 Graphical Description

The two-dimensional Gaussian wave packet solutions Eq. (6.2.9) are plotted with different incident parameters to graphically describe the time evolution of the scattering process, especially in the condition of selective adsorption. As shown in chapter 5, selective adsorption for the system used in this thesis occurs when

$$E_b = -\frac{mg^2}{2\hbar^2}, \quad (6.3.1)$$

where  $E_b$  is the bound state energy of the laterally averaged potential  $w(z) = -|g|\delta(z)$ . Thus, the two-dimensional kinematic condition for selective adsorption in terms of the incident angle  $\theta_i$  and the magnitude of the incident wave vector  $k_i$  is given by

$$\left(\sin \theta_i + \frac{2\pi}{ak_i}\right)^2 = 1 + \frac{m^2g^2}{\hbar^4k_i^2}. \quad (6.3.2)$$

If one of the energy levels of  $^1\text{H}_2$  - graphite system given in chapter 3 is used for  $E_b$ , the value of  $|g|$  corresponding to that energy level can be obtained. Then,  $\theta_i$  that satisfies the kinematic condition for selective adsorption can be obtained for a given value of  $k_i$ . Here the fourth energy level is used for the value of  $|g|$  because for the values of  $|g|$  corresponding lower energy levels the kinematic condition for selective adsorption is satisfied only with large incident angles ( $\theta_i > 45^\circ$ ) for any

values of  $k_i$ : the wave packet is considered with its initial width of  $20 \text{ \AA}$  in the range  $-150 \text{ \AA} \leq x \leq 150 \text{ \AA}$  and  $-150 \text{ \AA} \leq z \leq 150 \text{ \AA}$  so for large incident angles it starts too close from the interaction site. The value of  $|g|$  corresponding to the fourth energy level is  $3.96 \text{ meV}\cdot\text{\AA}$ . Thus, for  $k_i = 1.12 \text{ \AA}^{-1}$  corresponding particles at the temperature of  $10 \text{ }^\circ\text{K}$  the kinematic condition of selective adsorption is satisfied when  $\theta_i = 12.94^\circ$ . The diagram for the Gaussian wave packet at this incident angle is shown in Figure 6.1.

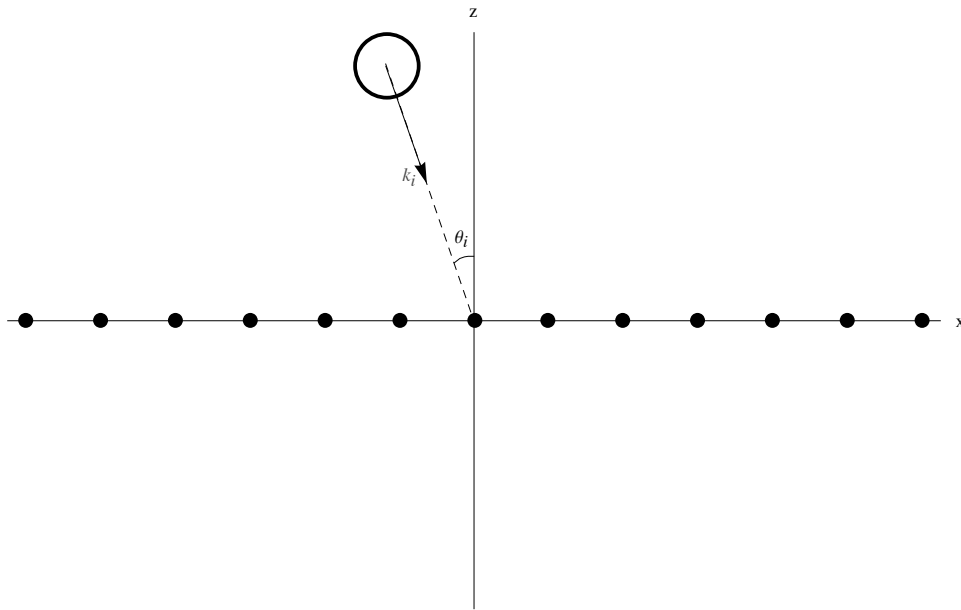


Fig 6.1. The diagram for computer simulation setup.  $k_i = 1.12 \text{ \AA}^{-1}$  and  $\theta_i = 12.94^\circ$ .

With the given values of  $|g|$  and  $k_i$ , the time evolution of the Gaussian wave packet at different incident angles are plotted:  $\theta_i = 12.94^\circ$ , which satisfies the kinematic condition of selective adsorption, in Figure 6.2, and those at other incident angles, which don't satisfy the kinematic condition of selective adsorption in Figure 6.3 and 6.4. In Figure 6.2 a faint line appears at  $z = 0$  where the periodic interaction site lies with the reflected and transmitted parts of the Gaussian wave packet after the interaction. However, the faint line doesn't appear in Figure 6.3 and 6.4, indicating this line is attributed to selective adsorption.

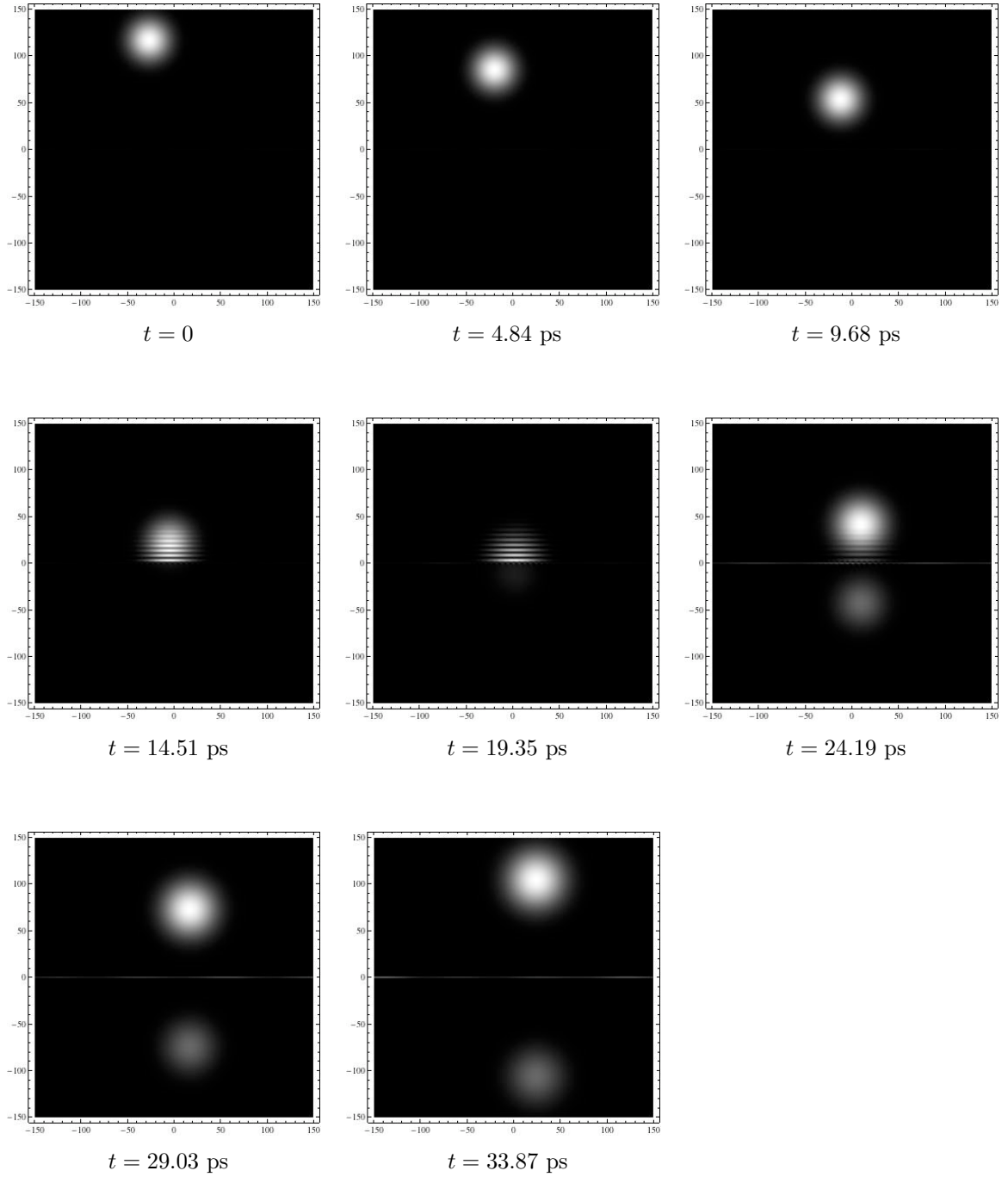


Fig 6.2. The density plots of the two-dimensional Gaussian wave packets at different times for  $^1\text{H}_2$  with  $|g| = 3.96 \text{ meV}\cdot\text{\AA}$ ,  $k_i = 1.12 \text{ \AA}^{-1}$  and  $\theta_i = 12.94^\circ$ . With these values the kinematic condition of selective adsorption is satisfied. The periodic potential site lies on  $z = 0$ , but is not shown.

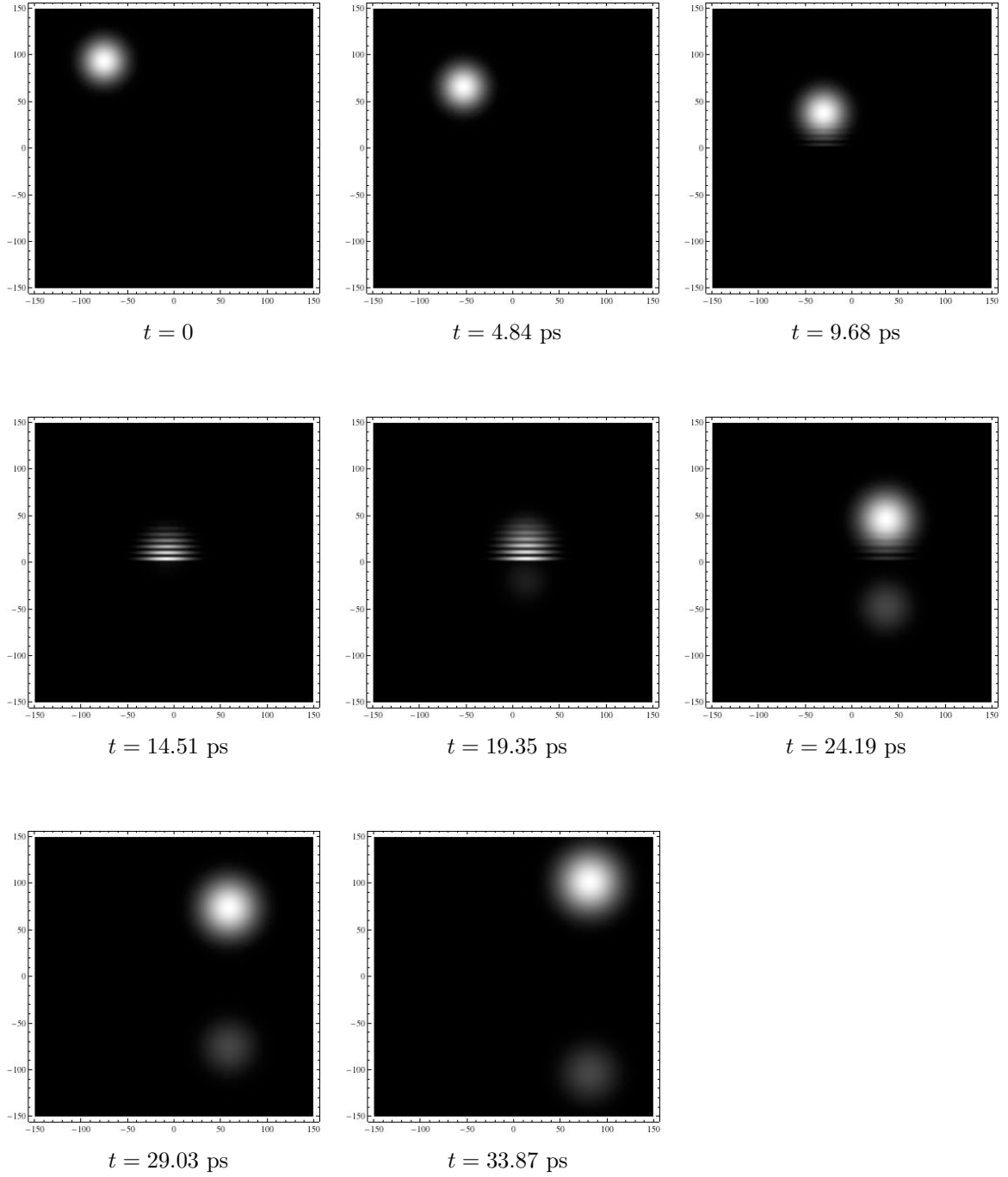


Fig 6.3. The density plots of the 2D Gaussian wave packets at different times for  $^1\text{H}_2$  with  $|g| = 3.96 \text{ meV}\cdot\text{\AA}$ ,  $k_i = 1.12 \text{ \AA}^{-1}$  and  $\theta_i = 38.82^\circ$ . This incident angle does not satisfy the kinematic condition of selective adsorption with the given values of  $|g|$  and  $k_i$ . The periodic potential site lies on  $z = 0$ , but is not shown.

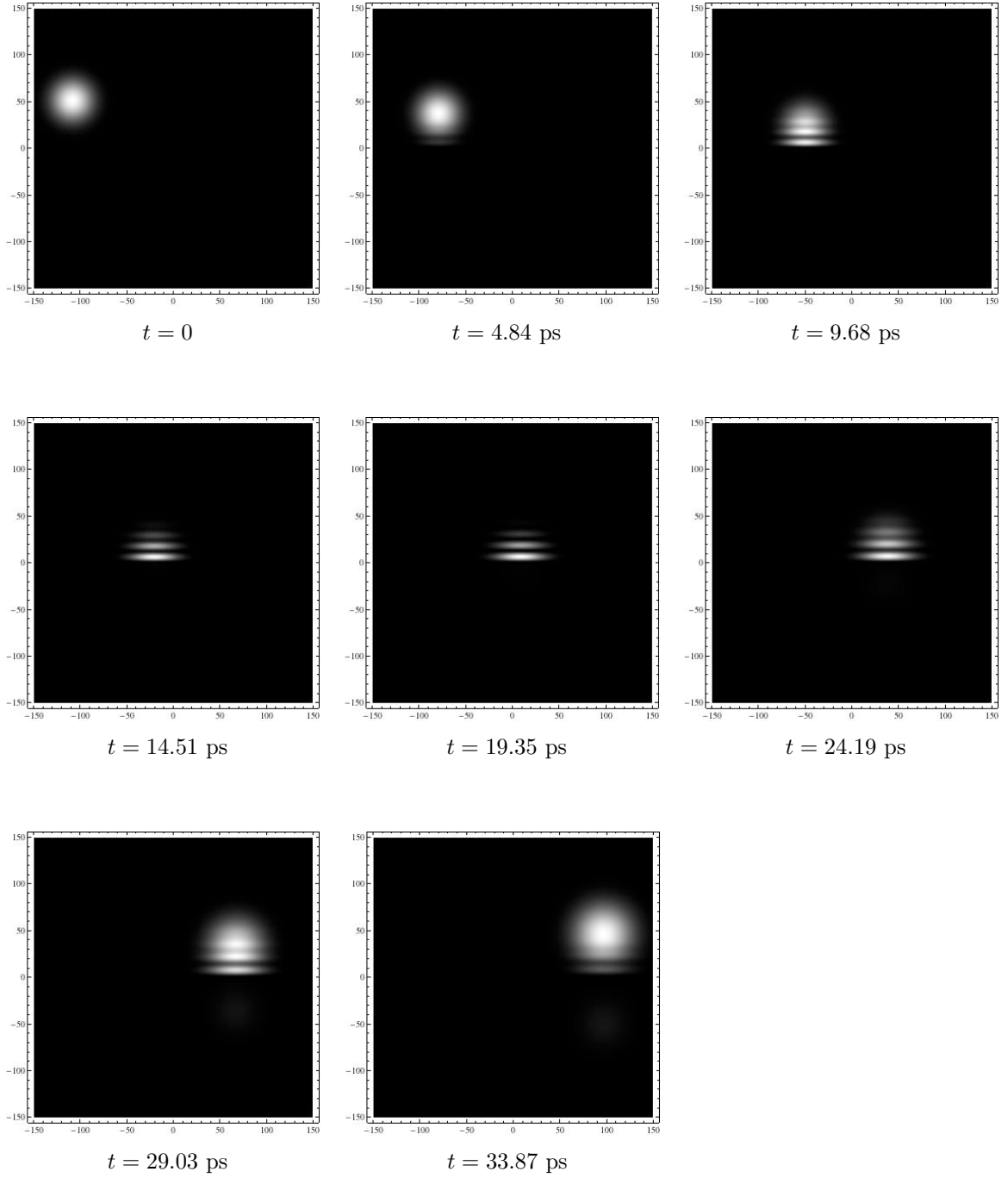


Fig 6.4. The density plots of the 2D Gaussian wave packets at different times for  $^1\text{H}_2$  with  $|g| = 3.96 \text{ meV}\cdot\text{\AA}$ ,  $k_i = 1.12 \text{ \AA}^{-1}$  and  $\theta_i = 64.70^\circ$ . This incident angle does not satisfy the kinematic condition of selective adsorption with the given values of  $|g|$  and  $k_i$ . The periodic potential site lies on  $z = 0$ , but is not shown.



## 6.4 Conclusions

We have treated the two-dimensional scattering of the gas-surface system with a model potential using a Gaussian wave packet approach to describe the time evolution of the scattering process, especially when the kinematic condition of selective adsorption is satisfied. Even with the simple model potential used in this thesis we have not been able to obtain an exact solution of a two-dimensional wave function from which a Gaussian wave packet can be constructed. Thus, we have constructed a Gaussian wave packet from a Born approximate wave function.

With this obtained Gaussian wave packet solution we have been able to depict the selective adsorption phenomenon, but unable to accurately determine the probability density of selectively adsorbed particles because the Gaussian wave packet constructed from the Born approximate wave function does not conserve the total probability density. In order to resolve this problem of non-conservation of the total probability density, we might attempt with the Born series as a future work.

APPENDIX A  
CALCULUS OF RESIDUES

The residue theorem states that

$$\oint_C f(z)dz = 2\pi i \sum \text{enclosed residues}, \quad (\text{A.1})$$

where the residue of  $f(z)$  with a pole of order  $m$  at  $z = z_0$  is given by [55]

$$a_{-1} = \frac{1}{(m-1)!} \frac{d^{m-1}}{dz^{m-1}} [(z-z_0)^m f(z)]_{z=z_0}. \quad (\text{A.2})$$

The residue theorem is very useful in evaluating definite integrals, as employed in the following integral

$$\int_{-\infty}^{\infty} dk' \frac{1}{k'^2 - k^2 - i\epsilon}, \quad (\text{A.3})$$

where  $k$  is a real number, and  $\epsilon$  is a positive real infinitesimal that will be set to zero. The integrand has two poles at  $k' = \pm\sqrt{k^2 + i\epsilon}$  as shown in Figure A. Since  $k^2 \gg \epsilon$ ,

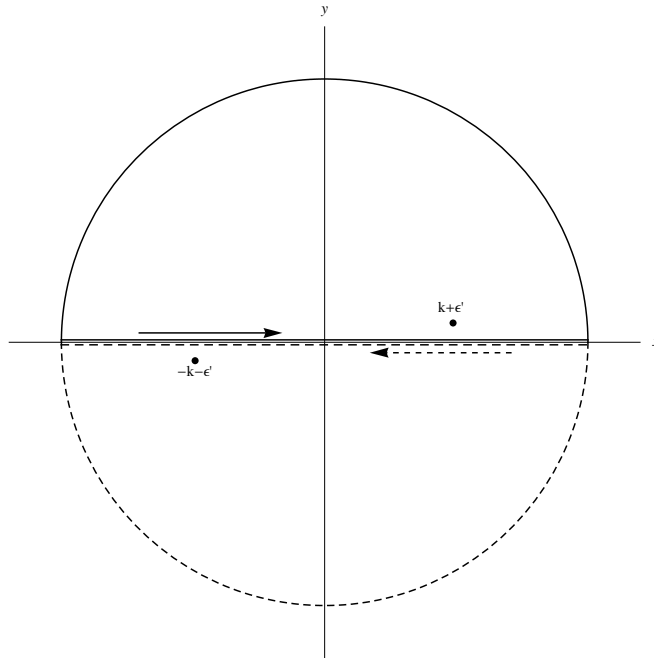


Fig A. Half circle contours.

Taylor's expansion of  $\sqrt{k^2 + i\epsilon}$  can be used. Thus, the residue in the upper half-plane is given by

$$a_{-1} = [k' - (k + i\epsilon')] \frac{1}{[k' + (k + i\epsilon)'][k' - (k + i\epsilon)']} \Big|_{k'=k+i\epsilon'} \stackrel{\epsilon' \rightarrow 0}{=} \frac{1}{2k}, \quad (\text{A.4})$$

where  $\epsilon' = k + i\frac{\epsilon}{2k}$ . Thus, the contour integral over  $dk'$  closed at infinity with a semicircle in the upper half-plane is given by

$$\int dk' \frac{1}{k'^2 - k^2 - i\epsilon} = 2\pi i a_{-1} = i\frac{\pi}{k}. \quad (\text{A.5})$$

It is also possible to use the lower half-plane, and this choice will lead to the same result.

## APPENDIX B

### BOUND-STATE WAVE FUNCTION FOR $\delta$ POTENTIAL

The Schrödinger equation for the delta function potential  $w_0(z) = -|g|\delta(z)$  is given by

$$-\frac{\hbar^2}{2m} \frac{d^2\psi(z)}{dz^2} - |g|\delta(z)\psi(z) = E\psi(z), \quad (\text{B.1})$$

where  $m$  and  $E$  are mass and the total energy of a particle, respectively. In the region  $z < 0$  the Schrödinger equation Eq. (B.1) is given by

$$\frac{d^2\psi(z)}{dz^2} = k^2\psi(z), \quad (\text{B.2})$$

where

$$k = \frac{\sqrt{-2mE}}{\hbar}. \quad (\text{B.3})$$

The general solution to Eq. (B.2) is given by

$$\psi(z) = Ae^{kz} + Be^{-kz}. \quad (\text{B.4})$$

For bound states ( $E < 0$ ) the second term grows exponentially without limit as  $z \rightarrow -\infty$ , so we should set  $B = 0$ . Thus,

$$\psi(z) = Ae^{kz}, \quad (z < 0). \quad (\text{B.5})$$

In the region  $z > 0$ , Eq. (B.1) becomes Eq. (B.2) again, and the general solution is given by

$$\psi(z) = Ce^{kz} + De^{-kz}. \quad (\text{B.6})$$

This time the first term grows exponentially without limit as  $z \rightarrow \infty$ , so we should set  $C = 0$ . Thus, we have

$$\psi(z) = De^{-kz}, \quad (z > 0). \quad (\text{B.7})$$

In order to obtain the coefficients  $A$  and  $D$ , the appropriate boundary conditions at  $z = 0$  need to be imposed. The first boundary condition is that the wave function is

continuous at  $z = 0$  so from Eq. (B.5) and Eq. (B.7) we have

$$A = D. \quad (\text{B.8})$$

The second boundary condition is the behavior of the derivative of the wave function at  $z = 0$ , which is obtained by integrating Eq. (B.1) over an interval  $[-\epsilon, +\epsilon]$  and then take the limit as  $\epsilon \rightarrow 0$ :

$$-\frac{\hbar^2}{2m} \int_{-\epsilon}^{+\epsilon} \frac{d^2\psi(z)}{dz^2} dz - |g| \int_{-\epsilon}^{+\epsilon} \delta(z)\psi(z) dz = E \int_{-\epsilon}^{+\epsilon} \psi(z) dz. \quad (\text{B.9})$$

The right-hand side of Eq. (B.9) vanishes in the limit  $\epsilon \rightarrow 0$ . Thus, Eq. (B.9) becomes

$$\lim_{\epsilon \rightarrow 0} \left[ \frac{d\psi(z)}{dz} \Big|_{+\epsilon} - \frac{d\psi(z)}{dz} \Big|_{-\epsilon} \right] = -\frac{2m|g|}{\hbar^2} \psi(0). \quad (\text{B.10})$$

Thus, using the result obtained from the first boundary condition Eq. (B.8) and the derivatives of the wave functions, Eq. (B.5) and Eq. (B.7), we obtain

$$k = \frac{m|g|}{\hbar^2}. \quad (\text{B.11})$$

The wave function is thus given by

$$\psi(z) = Ae^{-m|g||z|/\hbar^2}. \quad (\text{B.12})$$

The term  $A$  is obtained by normalizing the wave function such that

$$\begin{aligned} \int_{-\infty}^{+\infty} |\psi(z)|^2 dz &= |A|^2 \int_{-\infty}^0 e^{2kz} dz + |A|^2 \int_0^{+\infty} e^{-2kz} dz = \frac{|A|^2}{k} = 1 \\ \Rightarrow A &= \pm\sqrt{k} = \pm\frac{\sqrt{m|g|}}{\hbar}. \end{aligned} \quad (\text{B.13})$$

Therefore, the bound state wave function for the delta function potential is given by

$$\psi(z) = \pm\frac{\sqrt{m|g|}}{\hbar} e^{-m|g||z|/\hbar^2}. \quad (\text{B.14})$$

## APPENDIX C

### SOURCE CODE FOR NUMERICAL CALCULATION

The code is written in Fortran for parallel computing using Open MPI. The data types defined in Numerical Recipes [56] are adopted, and one of its functions *factrl*, which returns the result of the factorial operation, is used. The algorithm for Simpson's Rule is obtained from Dr. Pang [57].

This program returns the probability densities of the two-dimensional Gaussian wave packet obtained in chapter 6 with a modification of the initial position of the wave packet denoted by  $x_i$  and  $z_i$  in the code: in chapter 6 they are set to zero, and in the code they are adjusted with respect to the incident angle of the wave packet so that they are 120 Å away from the origin. It can run on multiple processors (even number): each processor computes and returns the probability densities of the wave packet at different points at a given time, and then the primary processor collects those probability densities and writes on a file called "density.dat".

File Name: gconst.f90

---

```
MODULE gconst
  USE nrtype
  REAL(DP), PARAMETER :: MU = 3701.38_dp, G = 0.000275_dp, &
    LMDA = 0.0000275_dp, HBAR = 1.0_dp
  REAL(DP), PARAMETER :: sigma_kx = 0.05_dp, sigma_x = 20.0_dp, &
    sigma_kz = 0.05_dp, sigma_z = 20.0_dp, &
    xi = -26.8718_dp, zi = 116.953_dp, site_dist = 6.0_dp
  COMPLEX(DPC), PARAMETER :: i = (0.0_dp, 1.0_dp)
END MODULE gconst
```

---

File Name: mpiwp.f90

---

```
PROGRAM mpiwp
  USE nrtype
  USE gconst
  IMPLICIT NONE
  INCLUDE "mpif.h"
  INTEGER(I4B), PARAMETER :: NSTEP = 513, XMAX = 150, ZMAX = 150, TMAX = 7
  REAL(DP), PARAMETER :: ki = 0.6_dp, theta = 12.9401_dp
  INTEGER(I4B) :: j
  REAL(DP) :: lower_kx_limit, upper_kx_limit, lower_kz_limit, upper_kz_limit, del_kx, del_kz, &
    kx, x, z, t, kxi, kzi, vxi, vzi, wxi, wzi, tau_x, tau_z, angle, coeff1
```

```

COMPLEX(DPC) :: coeff2, sumf, psix0, psiz0, psiz1, psixz
COMPLEX(DPC), DIMENSION(NSTEP) :: fkz_of_kx
INTEGER(I4B) :: my_rank, num_proc, src, dest, tag, ierr
INTEGER(I4B) :: status(3)
INTEGER(I4B) :: ti, local_ti, local_tf, local_tmax, arraysize, aerr, tm, xm, zm
REAL(DP), DIMENSION(:, :, :), ALLOCATABLE :: prob, tempa
INTERFACE
  FUNCTION func_kx(NSTEP, lower_kx.limit, del_kx, fkz_of_kx, kxi, x, t)
    USE nrtype
    USE gconst
    IMPLICIT NONE
    INTEGER(I4B), INTENT(IN) :: NSTEP
    REAL(DP), INTENT(IN) :: lower_kx.limit, del_kx, kxi, x, t
    INTEGER(I4B) :: j
    COMPLEX(DPC), INTENT(IN), DIMENSION(NSTEP) :: fkz_of_kx
    REAL(DP) :: kx, angle
    COMPLEX(DPC), DIMENSION(NSTEP) :: func_kx
  END FUNCTION func_kx
  FUNCTION func_kz(NSTEP, lower_kz.limit, del_kz, kzi, kx, x, z, t)
    USE nrtype
    USE gconst
    IMPLICIT NONE
    INTEGER(I4B), INTENT(IN) :: NSTEP
    REAL(DP), INTENT(IN) :: lower_kz.limit, del_kz, kzi, kx, x, z, t
    INTEGER(I4B) :: j
    REAL(DP) :: kz, sqrterm, angle
    COMPLEX(DPC), DIMENSION(NSTEP) :: func_kz
    COMPLEX(DPC) :: wc
  END FUNCTION func_kz
  FUNCTION intg_term(gmm)
    USE nrtype
    IMPLICIT NONE
    COMPLEX(DPC), INTENT(IN) :: gmm
    INTEGER(I4B) :: j, jj, prod
    COMPLEX(DPC) :: sumc, intg_term
  END FUNCTION intg_term
  FUNCTION gamma(kzi, z, t)
    USE nrtype
    USE gconst
    IMPLICIT NONE
    REAL(DP), INTENT(IN) :: kzi, z, t
    COMPLEX(DPC) :: gamma
  END FUNCTION gamma
END INTERFACE

dest = 0
tag = 1
CALL MPI_INIT(ierr)
CALL MPI_COMM_RANK(MPI_COMM_WORLD, my_rank, ierr)
CALL MPI_COMM_SIZE(MPI_COMM_WORLD, num_proc, ierr)

ti = 0
local_tmax = (TMAX+1) / num_proc
local_ti = ti + my_rank * local_tmax

```

```

local.tf = local.ti + local.tmax - 1

ALLOCATE(prob(0:TMAX, -XMAX:XMAX, -ZMAX:ZMAX), STAT = aerr)
IF (aerr /= 0) THEN
  PRINT *, "multiarray : allocation failed"
  STOP
END IF

angle = theta * PLD / 180.0_dp
kxi = ki * sin(angle)
kzi = ki * cos(angle)
vxi = HBAR * kxi / MU
vzi = HBAR * kzi / MU
wxi = HBAR * kxi * kxi / (2 * MU)
wzi = HBAR * kzi * kzi / (2 * MU)
tau_x = MU * sigma_x * sigma_x / HBAR
tau_z = MU * sigma_z * sigma_z / HBAR
lower_kx_limit = -3.0_dp
upper_kx_limit = 3.0_dp
lower_kz_limit = -3.0_dp
upper_kz_limit = 3.0_dp
del_kx = (upper_kx_limit - lower_kx_limit) / (NSTEP - 1)
del_kz = (upper_kz_limit - lower_kz_limit) / (NSTEP - 1)
coeff1 = sqrt(sigma_x * sigma_x) / (2 * PLD)
coeff2 = -i * MU * LMDA / (4 * PLD * sqrt(sigma_kx * sigma_kz * PLD))

DO tm = local.ti, local.tf
  t = tm * 200000.0_dp
  DO xm = -XMAX, XMAX
    x = xm * 1.0_dp
    psix0 = sqrt(2*PLD)/(sigma_x*sqrt(1 + i*t/tau_x))*exp(i*(kxi*x - kxi*xi - wxi*t)) &
      *exp(-(x - xi - vxi*t)**2/(2*sigma_x*sigma_x*(1 + i*t/tau_x)))
    DO zm = -ZMAX, ZMAX
      z = zm * 1.0_dp
      psiz0 = sqrt(2*PLD)/(sigma_z*sqrt(1 + i*t/tau_z))*exp(-i*(kzi*z - kzi*zi + wzi*t)) &
        *exp(-(z - zi + vzi*t)**2/(2*sigma_z*sigma_z*(1 + i*t/tau_z)))
      psiz1 = i*MU*abs(G)/(HBAR*HBAR)*exp(i*(kzi*abs(z) + kzi*zi - wzi*t)) &
        *exp(-(abs(z) + zi - vzi*t)**2/(2*sigma_z*sigma_z*(1 + i*t/tau_x))) &
        *intg_term(gamma(kzi, z, t))
      DO j = 1, NSTEP
        kx = lower_kx_limit + del_kx * (j-1)
        sumf = simpson(NSTEP, del_kz, func_kz(NSTEP, lower_kz_limit, del_kz, kzi, kx, &
          x, z, t))
        fkz_of_kx(j) = sumf
      END DO
      sumf = simpson(NSTEP, del_kx, func_kx(NSTEP, lower_kx_limit, del_kx, fkz_of_kx, &
        kxi, x, t))
      psixz = coeff1*(psix0*psiz0 + psix0*psiz1) + coeff2*sumf
      prob(tm, xm, zm) = abs(psixz)**2
    END DO
  END DO
END DO

arraysize = num_proc*(local.tmax)*(2*XMAX + 1)*(2*ZMAX + 1)

```



```

IF(my_rank == 0) THEN
  ALLOCATE(tempa(0:TMAX, -XMAX:XMAX, -ZMAX:ZMAX), STAT = aerr)
  IF (aerr /= 0) THEN
    PRINT *, "tempa : allocation failed."
    STOP
  END IF
  tempa = prob
  DO src = 1, num_proc - 1
    CALL MPI_RECV(prob, arraysize, MPI_DOUBLE_PRECISION, src, tag, &
                  MPI_COMM_WORLD, status, ierr)
    tempa = tempa + prob
  END DO
  prob = tempa
  DEALLOCATE(tempa)
ELSE
  CALL MPI_SEND(prob, arraysize, MPI_DOUBLE_PRECISION, dest, tag, &
                MPI_COMM_WORLD, ierr)
END IF

IF(my_rank == 0) THEN
  OPEN(UNIT = 2, FILE = "density.dat")
  DO tm = 0, TMAX
    DO xm = -XMAX, XMAX
      DO zm = -ZMAX, ZMAX
        WRITE(2, "(3I8, F24.16)") tm, xm, zm, prob(tm, xm, zm)
      END DO
    END DO
  END DO
  CLOSE(2)
END IF
DEALLOCATE(prob)
CALL MPI_FINALIZE(ierr)
END PROGRAM mpiwp

FUNCTION func_kx(NSTEP, lower_kx_limit, del_kx, fkz_of_kx, kxi, x, t)
  USE nrtype
  USE gconst
  IMPLICIT NONE
  INTEGER(I4B), INTENT(IN) :: NSTEP
  REAL(DP), INTENT(IN) :: lower_kx_limit, del_kx, kxi, x, t
  INTEGER(I4B) :: j
  COMPLEX(DPC), INTENT(IN), DIMENSION(NSTEP) :: fkz_of_kx
  REAL(DP) :: kx
  COMPLEX(DPC), DIMENSION(NSTEP) :: func_kx

  DO j = 1, NSTEP
    kx = lower_kx_limit + del_kx*(j-1)
    func_kx(j) = exp(-(kx-kxi)**2/(2*sigma_kx*sigma_kx))*exp(-i*HBAR*kx*kx*t/(2*MU)) &
                *exp(i*kx*(x - xi))*fkz_of_kx(j)
  END DO
END FUNCTION func_kx

FUNCTION func_kz(NSTEP, lower_kz_limit, del_kz, kzi, kx, x, z, t)
  USE nrtype

```

```

USE gconst
IMPLICIT NONE
INTEGER(I4B), INTENT(IN) :: NSTEP
REAL(DP), INTENT(IN) :: lower_kz_limit, del_kz, kzi, kx, x, z, t
INTEGER(I4B) :: j
REAL(DP) :: kz, sqrterm_p, sqrterm_m
COMPLEX(DPC), DIMENSION(NSTEP) :: func_kz
COMPLEX(DPC) :: wc_p, wc_m, fkz1, fkz2, fkz3

DO j = 1, NSTEP
  kz = lower_kz_limit + del_kz*(j-1)
  sqrterm_m = (kz*kz) - (4*PI.D/site.dist)*(kx + PI.D/site.dist)
  sqrterm_p = (kz*kz) + (4*PI.D/site.dist)*(kx - PI.D/site.dist)
  IF( sqrterm_m < 0.0_dp ) THEN
    sqrterm_m = -1.0_dp * sqrterm_m
    wc_m = cmplx(0.0_dp, sqrt(sqrterm_m))
  ELSE
    wc_m = cmplx(sqrt(sqrterm_m), 0.0_dp)
  END IF
  IF( sqrterm_p < 0.0_dp ) THEN
    sqrterm_p = -1.0_dp * sqrterm_p
    wc_p = cmplx(0.0_dp, sqrt(sqrterm_p))
  ELSE
    wc_p = cmplx(sqrt(sqrterm_p), 0.0_dp)
  END IF
  fkz1 = HBAR*HBAR*kz/(HBAR*HBAR*kz - i*MU*abs(G)) &
    *exp(-(kz - kzi)**2/(2*sigma_kz*sigma_kz))*exp(-i*HBAR*kz*kz*t/(2*MU))
  fkz2 = exp(i*2*PI.D*x/site.dist)*exp(i*wc_m*abs(z))/(HBAR*HBAR*wc_m - i*MU*abs(G))
  fkz3 = exp(-i*2*PI.D*x/site.dist)*exp(i*wc_p*abs(z))/(HBAR*HBAR*wc_p - i*MU*abs(G))
  func_kz(j) = fkz1 * (fkz2 + fkz3)
END DO
END FUNCTION func_kz

FUNCTION simpson(NSTEP, del, fi)
  USE nrtype
  IMPLICIT NONE
  INTEGER(I4B) :: j
  INTEGER(I4B), INTENT(IN) :: NSTEP
  REAL(DP), INTENT(IN) :: del
  COMPLEX(DPC) :: f0, f1, f2, simp, simpson
  COMPLEX(DPC), INTENT(IN), DIMENSION (NSTEP) :: fi

  simp = (0.0_dp, 0.0_dp)
  f0 = (0.0_dp, 0.0_dp)
  f1 = (0.0_dp, 0.0_dp)
  f2 = (0.0_dp, 0.0_dp)
  DO j = 2, NSTEP - 1, 2
    f0 = f0 + fi(j)
    f1 = f1 + fi(j - 1)
    f2 = f2 + fi(j + 1)
  END DO
  simp = del * (f1 + 4.0_dp * f0 + f2) / 3.0_dp
  IF (MOD(NSTEP, 2) = 0) THEN
    simp = simp + del*(5.0_dp*fi( NSTEP) + 8.0_dp*fi(NSTEP - 1) - fi(NSTEP - 2))/12.0_dp
  
```

```

    END IF
    simpson = simp
END FUNCTION simpson

FUNCTION cerfc(cz)
    USE nrtype
    USE nr, ONLY : factrl
    IMPLICIT NONE
    COMPLEX(DPC), INTENT(IN) :: cz
    COMPLEX(DPC) :: zz, sumc, cerfc
    INTEGER(I4B) :: j
    REAL(DP) :: real_cz, abs_cz

    zz = cz
    real_cz = real(cz)
    abs_cz = abs(cz)
    sumc = (0.0_dp, 0.0_dp)
    IF (real_cz < 0) THEN
        zz = - cz
    END IF
    IF (abs_cz < 4.5_dp) THEN
        DO j = 0, 100
            sumc = sumc + (-1)**j * zz**(2 * j + 1) / (factrls(j) * (2 * j + 1))
        END DO
        IF (real_cz < 0) THEN
            cerfc = (1.0_dp, 0.0_dp) + 2 / sqrt(PI_D) * sumc
        ELSE
            cerfc = (1.0_dp, 0.0_dp) - 2 / sqrt(PI_D) * sumc
        END IF
    ELSE
        DO j = 0, 10
            sumc = sumc + (-1)**j * factrls(2 * j) / (factrls(j) * (2 * zz)**(2 * j))
        END DO
        IF (real_cz < 0) THEN
            cerfc = (2.0_dp, 0.0_dp) - exp(-zz * zz) / (zz * sqrt(PI_D)) * sumc
        ELSE
            cerfc = exp(-zz * zz) / (zz * sqrt(PI_D)) * sumc
        END IF
    END IF
END FUNCTION cerfc

FUNCTION intg_term(gmm)
    USE nrtype
    IMPLICIT NONE
    COMPLEX(DPC), INTENT(IN) :: gmm
    INTEGER(I4B) :: j, jj, prod
    COMPLEX(DPC) :: sumc, intg_term
    INTERFACE
        FUNCTION cerfc(cz)
            USE nrtype
            IMPLICIT NONE
            COMPLEX(DPC), INTENT(IN) :: cz
            COMPLEX(DPC) :: zz, sumc, cerfc
            INTEGER(I4B) :: j

```

```

        REAL(DP) :: real_cz, abs_cz
    END FUNCTION cerfc
END INTERFACE

sumc = (0.0_dp, 0.0_dp)
IF(abs(gmm) > 5.0_dp) THEN
    DO j = 1, 10
        prod = 1
        DO jj = 1, j
            prod = prod * (2 * jj - 1)
        END DO
        sumc = sumc + (-1)**j * prod / (-2 * gmm * gmm)**j
    END DO
    intg_term = sqrt(PLD) / gmm * (1 + sumc)
ELSE
    intg_term = -gmm * sqrt(-1 / (gmm * gmm)) * exp(-gmm * gmm) * PLD &
        * cerfc(-gmm * gmm * sqrt(-1 / (gmm * gmm)))
END IF
END FUNCTION intg_term

FUNCTION gamma(kzi, z, t)
    USE nrtype
    USE gconst
    IMPLICIT NONE
    REAL(DP), INTENT(IN) :: kzi, z, t
    COMPLEX(DPC) :: gamma

    gamma = 1 / sqrt(2.0_dp) * ( i * (abs(z) + zi - HBAR * kzi * t / MU) &
        / (sigma_z * sqrt(1 + i * HBAR * t / (MU * sigma_z * sigma_z))) &
        + (kzi - i * MU * abs(G) / (HBAR * HBAR)) * sigma_z &
        * sqrt(1 + i * HBAR * t / (MU * sigma_z * sigma_z)))
END FUNCTION gamma

```

---

## BIBLIOGRAPHY

- [1] H. G. Schimmel, G. J. Kearley, M. G. Nijkamp, C. T. Visser, K. P. de Jong, and F. M. Mulder, "Hydrogen adsorption in carbon nanostructures: Comparison of nanotubes, fibers, and coals," *Chem. Eur. J.*, vol. 9, pp. 4764–4770, 2003.
- [2] I. Cabria, M. J. Lopez, and J. A. Alonso, "Enhancement of hydrogen physisorption on graphene and carbon nanotubes by Li doping," *J. Chem. Phys.*, vol. 123, p. 204721, 2005.
- [3] D. Henwood and J. D. Carey, "Ab initio investigation of molecular hydrogen physisorption on graphene and carbon nanotubes," *Phys. Rev. B*, vol. 75, p. 245413, 2007.
- [4] B. Sakintuna, F. Lamari-Darkrim, and M. Hirscher, "Metal hydride materials for solid hydrogen storage: A review," *Int. J. Hydrogen Energy*, vol. 32, pp. 1121–1140, 2007.
- [5] A. C. Dillon, K. M. Jones, T. A. Bekkedahl, C. H. Kiang, D. S. Bethune, and M. J. Heben, "Storage of hydrogen in single-walled carbon nanotubes," *Nature*, vol. 386, pp. 377–379, 1997.
- [6] A. Chambers, C. Park, R. T. K. Baker, and N. M. Rodriguez, "Hydrogen storage in graphite nanofibers," *J. Phys. Chem. B*, vol. 102, no. 22, pp. 4253–4256, 1998.
- [7] C. Park, P. E. Anderson, A. Chambers, C. D. Tan, R. Hidalgo, and N. M. Rodriguez, "Further studies of the interaction of hydrogen with graphite nanofibers," *J. Phys. Chem. B*, vol. 103, pp. 10572–10581, 1999.
- [8] P. Chen, X. Wu, J. Lin, and K. L. Tan, "High H<sub>2</sub> uptake by alkali-doped nanotubes under ambient pressure and moderate temperatures," *Science*, vol. 285, no. 5424, pp. 91–93, 1999.
- [9] C. C. Ahn, Y. Ye, B. V. Ratnakumar, C. Witham, R. C. Bowman, Jr., and B. Fultz, "Hydrogen desorption and adsorption measurements on graphite nanobers," *Appl. Phys. Lett.*, vol. 73, no. 23, pp. 3378–3380, 1998.
- [10] F. E. Pinkerton, B. G. Wicke, C. H. Olk, G. G. Tibbetts, G. P. Meisner, M. S. Meyer, and J. F. Herbst, "Thermogravimetric measurement of hydrogen absorption in alkali-modified carbon materials," *J. Phys. Chem. B*, vol. 104, pp. 9460–9467, 2000.
- [11] M. Hirscher, M. Becher, M. Haluska, U. Dettlaff-Weglikowska, A. Quintel, G. S. Duesberg, Y. M. Choi, P. Downes, M. Hulman, S. Roth, I. Stepanek, and P. Bernier, "Hydrogen storage in sonicated carbon materials," *Appl. Phys. A*, vol. 72, pp. 129–132, 2001.

- [12] P. A. Gordon and R. B. Saeger, "Molecular modeling of adsorptive energy storage: Hydrogen storage in single-walled carbon nanotubes," *Ind. Eng. Chem. Res.*, vol. 38, pp. 4647–4655, 1999.
- [13] H. Dodziuk and G. Dolgonos, "Molecular modeling study of hydrogen storage in carbon nanotubes," *Chem. Phys. Letters*, vol. 356, pp. 79–83, 2002.
- [14] M. Rzepka, P. Lamp, and M. A. de la Casa-Lillo, "Physisorption of hydrogen on microporous carbon and carbon nanotubes," *J. Phys. Chem. B*, vol. 102, pp. 10894–10898, 1998.
- [15] R. F. Cracknell, "Molecular simulation of hydrogen adsorption in graphitic nanofibres," *Phys. Chem. Chem. Phys.*, vol. 3, pp. 2091–2097, 2001.
- [16] H. Hoinkes, H. Nahr, and H. Wilsch, "Surface debye temperature by atomic beam scattering," *Surface Sci.*, vol. 33, pp. 516–524, 1972.
- [17] M. W. Cole and D. R. Frankl, "Atomic and molecular beam scattering from crystal surfaces in the quantum regime," *Surface Sci.*, vol. 70, pp. 585–616, 1978.
- [18] A. Tsuchida, "Scattering of molecules by a crystal surface," *Surface Sci.*, vol. 14, pp. 375–394, 1969.
- [19] A. F. Devonshire, "The interaction of atoms and molecules with solid surfaces V – the diffraction and reflexion of molecular rays," *Proc. Roy. Soc. A*, vol. 156, pp. 37–44, 1936.
- [20] J. E. Lennard-Jones and A. F. Devonshire, "The interaction of atoms and molecules with solid surfaces VI – the behaviour of adsorbed helium at low temperatures," *Proc. Roy. Soc. A*, vol. 158, pp. 242–252, 1937.
- [21] J. E. Lennard-Jones and A. F. Devonshire, "The interaction of atoms and molecules with solid surfaces VII – the diffraction of atoms by a surface," *Proc. Roy. Soc. A*, vol. 158, pp. 253–268, 1937.
- [22] H. Hoinkes, H. Nahr, and H. Wilsch, "Reflection, diffraction and selective adsorption of atomic hydrogen on the (001) surface of LiF," *Surface Sci.*, vol. 30, pp. 363–378, 1972.
- [23] H. U. Finzel, H. Frank, H. Hoinkes, M. Luschka, H. Nahr, H. Wilsch, and U. Wonka, "Atom-surface scattering with velocity-selected H and D atomic beams from LiF and NaF (001)," *Surface Sci.*, vol. 49, pp. 577–605, 1975.
- [24] H. Frank, H. Hoinkes, and H. Wilsch, "Interaction of neutral hydrogen atoms with KCl (001)," *Surface Sci.*, vol. 63, pp. 121–142, 1977.
- [25] G. Derry, D. Wesner, S. Krishnaswamy, and D. Frankl, "Selective adsorption of  $^3\text{He}$  and  $^4\text{He}$  on clean surfaces of NaF and LiF," *Surface Sci.*, vol. 74, pp. 245–258, 1978.

- [26] G. Derry, D. Wesner, W. Carlos, and D. Frankl, "Selective adsorption of  $^3\text{He}$  and  $^4\text{He}$  on the basal plane surface of graphite," *Surface Sci.*, vol. 87, pp. 629–642, 1979.
- [27] L. Mattera, F. Rosatelli, C. Salvo, F. Tommasini, U. Valbusa, and G. Vidali, "Selective adsorption of  $^1\text{H}_2$  and  $^2\text{H}_2$  on the (0001) graphite surface," *Surface Sci.*, vol. 93, pp. 515–525, 1980.
- [28] A. Luntz, L. Mattera, M. Rocca, F. Tommasini, and U. Valbusa, "Accurate He – Ag (110) interaction potential determination by selective adsorption," *Surface Sci.*, vol. 120, pp. L447–L452, 1982.
- [29] W. Y. Leung, J. Z. Larese, and D. R. Frankl, "Selective adsorption of  $^4\text{He}$  on the NaCl (001) surface," *Surface Sci.*, vol. 136, pp. 649–662, 1984.
- [30] J. G. Wolken, "Theoretical studies of atom-solid elastic scattering: He+LiF," *J. Chem. Phys.*, vol. 58, pp. 3047–3064, 1973.
- [31] N. Cabrera, V. Celli, F. O. Goodman, and R. Manson, "Scattering of atoms by solid surfaces I," *Surface Sci.*, vol. 19, pp. 67–92, 1970.
- [32] G. Armand and J. R. Manson, "Scattering of neutral atoms by an exponential corrugated potential," *Phys. Rev. Letters*, vol. 43, pp. 1839–1842, 1979.
- [33] U. Garibaldi, A. C. Levi, R. Spadacini, and G. E. Tommei, "Quantum theory of atom-surface scattering: diffraction and rainbow," *Surface Sci.*, vol. 48, pp. 649–675, 1974.
- [34] J. A. Barker and D. J. Auerbach, "Gas-surface interactions and dynamics: thermal energy atomic and molecular mean studies," *Surface Sci. Rep.*, vol. 4, pp. 1–99, 1985.
- [35] F. O. Goodman, "Scattering of atoms by solid surfaces II. calculations for the elastic scattering of  $^3\text{He}$  and  $^4\text{He}$  by LiF," *Surface Sci.*, vol. 19, pp. 93–108, 1970.
- [36] A. Tsuchida, "Calculations of elastic scattering of He atoms by a pairwise interaction with a LiF(001) crystal surface," *Surface Sci.*, vol. 46, pp. 611–624, 1974.
- [37] H. Chow and E. D. Thompson, "Diffraction and selective adsorption in the corrugated hard wall model," *Surface Sci.*, vol. 54, pp. 269–292, 1976.
- [38] J. C. Crews, "Scattering of Helium and Argon from the cleavage plane of Lithium Fluoride," *J. Chem. Phys.*, vol. 37, pp. 2004–2008, 1962.
- [39] D. R. O'Keefe, J. J. N. Smith, R. L. Palmer, and H. Saltsburg, "Intensity data for the reflection and diffraction of  $^3\text{He}$ ,  $^4\text{He}$ ,  $\text{H}_2$  and  $\text{D}_2$  from the (001) surface of LiF," *Surface Sci.*, vol. 20, pp. 27–43, 1969.

- [40] B. R. Williams, “Scattering of helium atoms by phonons in the (001) surface of LiF at 150°k,” *J. Chem. Phys.*, vol. 55, pp. 3220–3235, 1971.
- [41] G. Boato, P. Cantini, U. Garibaldi, A. C. Levi, L. Mattera, T. Spadacini, and G. E. Tommei, “Diffraction and rainbow in atom-surface scattering,” *J. Phys. C*, vol. 6, pp. L394–L398, 1973.
- [42] J. Meyers and D. Frankl, “Selective adsorption of  $^4\text{He}$  on clean LiF (001) surfaces,” *Surface Sci.*, vol. 51, pp. 61–74, 1975.
- [43] J. J. Sakurai, *Modern Quantum Mechanics*. Addison-Wesley, revised ed., 1994.
- [44] W. A. Steele, *The Interaction of Gases with Solid Surfaces*. Pergamon, first ed., 1974.
- [45] H. Chow and E. D. Thompson, “Bound state resonances in atom-solid scattering,” *Surface Sci.*, vol. 59, pp. 225–251, 1976.
- [46] L. Mattera, C. Salvo, S. Terreni, and F. Tommasini, “A simple and flexible atom-surface potential with easy-to-handle vibrational spectrum,” *Surface Sci.*, vol. 97, pp. 158–170, 1980.
- [47] F. Boronde, C. Jaffé, and S. Miret-Artés, “Classical chaotic elastic atom-surface scattering,” *Surface Sci.*, vol. 317, pp. 211–220, 1994.
- [48] J. P. Toennies, W. Welz, and G. Wolf, “Molecular beam scattering studies of orbiting resonances and the determination of van der waals potentials for H-Ne, Ar, Kr, and Xe and for H<sub>2</sub>-Ar, Kr, and Xe,” *J. Chem. Phys.*, vol. 71, pp. 614–642, 1979.
- [49] S. I. Sandler and J. K. Wheatley, “Intermolecular potential parameter combining rules for the lennard-jones 6 -12 potential,” *Chem. Phys. Letters*, vol. 10, pp. 375–378, 1971.
- [50] A. Crowell and J. Brown, “Laterally averaged interaction potentials for  $^1\text{H}_2$  and  $^2\text{H}_2$  on the (0001) graphite surface,” *Surface Sci.*, vol. 123, pp. 296–304, 1982.
- [51] K. J. McCann and V. Celli, “A semiclassical treatment of atom-surface scattering: He + LiF (001),” *Surface Sci.*, vol. 61, pp. 10–24, 1976.
- [52] *Mathematica*. Wolfram Research, Inc., 6.0 ed., 2007.
- [53] C. Kittel, *Introduction to Solid State Physics*. Wiley, seven ed., 2007.
- [54] D. Levin, “Procedures for computing one- and two-dimensional integrals of functions with rapid irregular oscillations,” *Mathematics of Computation*, vol. 38, pp. 531–538, 1982.
- [55] G. B. Arfken and H. J. Weber, *Mathematical Methods For Physicists*. Elsevier, sixth ed., 2005.



- [56] W. H. Press, S. A. Teukolsky, W. T. Vetterling, and B. P. Flannery, *Numerical Recipes in Fortran 90: The Art of Scientific Computing*. Cambridge University Press, second ed., 1986.
- [57] T. Pang, *An Introduction to Computational Physics*. Cambridge University Press, second ed., 2006.

VITA

Graduate College  
University of Nevada, Las Vegas

Michael Sohn

Home Address:

9113 Big Plantation Avenue  
Las Vegas, Nevada 89143

Degrees:

Bachelor of Science, Physics, 2007  
University of Nevada, Las Vegas

Thesis Title: Theoretical and Computational Study of Time Dependent Scattering  
on a 2D Surface

Thesis Examination Committee:

Chairperson, Bernard Zygelman, Ph. D.  
Committee Member, Tao Pang, Ph. D.  
Committee Member, Stephen Lepp, Ph. D.  
Graduate Faculty Representative, Kathleen A. Robins, Ph. D.